Chelating 3*H*-1,2,3,4-Triazaphospholes: Synthesis and Coordination Chemistry of Novel Bidentate Ligands Based on Low-Coordinate Phosphorus Heterocycles

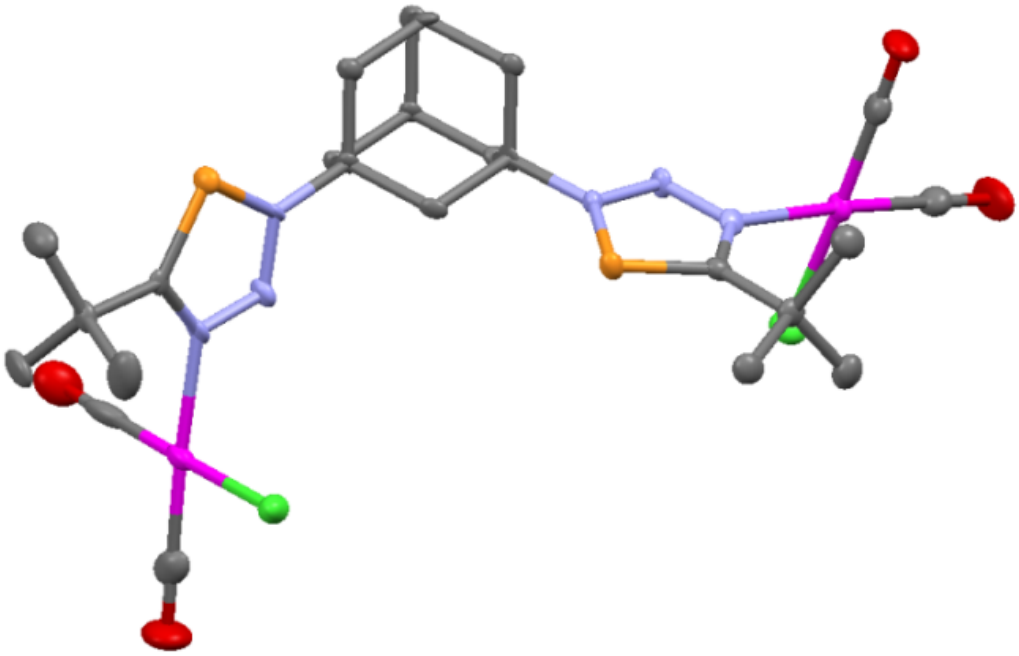

Author: Annette B. Vliegenthart B.Sc.
Supervisor (FU): Prof. Dr. C. Müller
Supervisors (UU): Prof.Dr. R.J.M. Klein Gebbink and Dr. M-E. Moret
October 2015 - March 2016
Institute for Chemistry and Biochemistry

Universiteit Utrecht

Freie Universität Berlin

Abstract

Two different synthetic pathways were investigated for the synthesis of new substituted 3*H*-1,2,3,4-triazaphospholes. These compounds may be synthesized through a [3+2] cycloaddition reaction between a phospaalkyne and an azide. In the first pathway, the diphosphaalkyne **22** was synthesized by varying several reaction conditions. However, compound **22** could not be obtained.

During the second pathway, the diazide **23** was synthesized instead of phosphaalkyne **22**. Different phosphaalkynes were used in [3+2] cycloaddition reactions with diazide **23**, and three new 3*H*-1,2,3,4-triazaphosphole derivatives were obtained. Two of them (compounds **32** and **35**) were purified and characterized. The bidentate properties of these two compounds were investigated in coordination chemistry.

Metal complexation reactions were performed with several metal precursors, e.g. Cu(I), Au(I) and Rh(I). A new complex is formed only in the case of Rh(I). The complexation of compound **32** with $[Rh(CO)_2Cl]_2$ (2:1 ratio) results in complex **40**. The dimer dissociates and coordinates via the N^1 atoms of the 3*H*-1,2,3,4-triazaphosphole arms.

For ligand **32**, no bidentate properties were exhibited. Different metals (e.g. Ir or Ag) or ligand modification may result in bidentate behavior.

Table of Content

List of abbreviations

^{1}H NMR	proton Nuclear Magnetic Resonance
^{13}C NMR	carbon Nuclear Magnetic Resonance
^{15}N NMR	nitrogen Nuclear Magnetic Resonance
DCM	dichloromethane
DABCO	1,4-diazabicyclo[2.2.2]octane
ESI-MS	Electron Spray Ionization - Mass Spectrometry
g	gram
h	hour
HASB	hard acids and soft bases
J	coupling constant
Mes*-	1,3,5-(Tri-tert-butyl)benzol
mg	milligram
MHz	mega Hertz
Hz	Hertz
m/z	mass over charge
ppm	parts per million
r.t.	room temperature
TAP	3*H*-1,2,3,4-triazaphosphole
THF	tetrahydrofuran
TMS	trimethylsilyl
XRD	X-ray Diffraction

1. Theory

1.1 Classical phosphorus compounds

Phosphorus(III) compounds play an important role in chemistry. A few examples of areas in which they appear are biochemistry, organic chemistry and materials science.[1] Furthermore, these compounds are also used as ligands in homogeneous catalysis.[2] In this field, they are usually known as a $\lambda^3\sigma^3$-phosphorus compounds or as classical phosphorus compounds, which has a coordination number of three (Figure 1). The R groups vary widely, which influences the electronic and steric properties of the ligand.[2] The properties of the ligand can be finely tuned, which impacts the catalytic properties of the complex.

1.2 Low-coordinate phosphorus(III) compounds

Recently, low-coordinate phosphorus compounds have again attracted attention. They are all trivalent with a coordination number of two (λ^3- σ^2) or one (λ^3- σ^1).[3] Figure 1 shows an overview of the different phosphorus compounds classes.

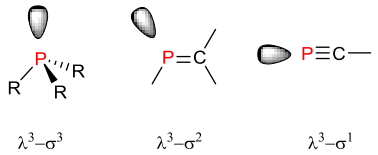

Figure 1: An overview of the different phosphorus compounds classes.[3]

P=C bonds are reactive, but can be stabilized by incorporation into an aromatic system.[4,5] This opens up a new class of phosphorus compounds, since they have different electronic and steric properties compared to classical ones.[4,5] Figure 2 shows a few examples where they are incorporated into an aromatic system. Compound **1** and **2** have conjugated π-systems and contain only phosphorus, carbon and hydrogen. Compound **3** and **4** incorporate nitrogen atoms into the aromatic ring. Compound **4**, a 3*H*-1,2,3,4-triazaphosphole derivative, has a highly conjugated system due to the three nitrogen atoms. This report will focus on 3*H*-1,2,3,4-triazaphosphole (TAP) derivatives.

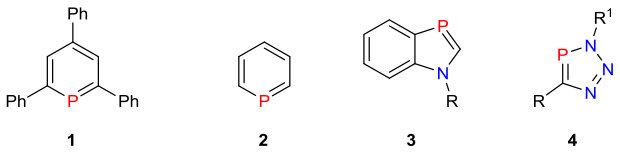

Figure 2: A selection of low-coordinate phosphorus compounds.[4]

1.3 Synthesis of 3*H*-1,2,3,4-triazaphosphole derivatives

The synthesis of compound **4** is derived from the Huisgen [3+2] cycloaddition reaction (Scheme 1).[6] This reaction occurs between an azide and alkyne. Unfortunately, this reaction is not selective. A mixture of 1,4- and 1,5-regioisomers are obtained (Scheme 1). Selectivity can be obtained by adding a catalyst. A copper-catalyzed azide-alkyne cycloaddition (CuAAC) can be performed for obtaining the 1,4-isomer (Scheme 1).[7] This reaction is also known as a "click" reaction. The 1,5-isomer can also selectively be obtained using a Ru-catalyst.[8]

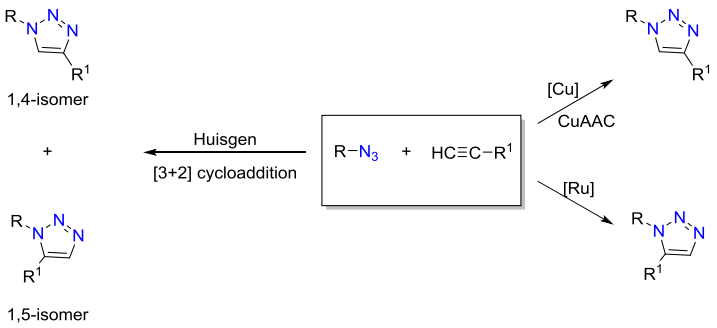

Scheme 1: Huisgen [3+2] cycloaddition (left) and the selective formation of the 1,4-and 1,5-isomer using a catalyst (right). For the 1,4-isomer, a copper catalyst was used, while a ruthenium catalyst was needed for the 1,5-isomer.[4]

For the 1,4-product, a catalytic cycle was described by Fokin *et al.*[9] Scheme 2 showed the proposed reaction mechanism, which was determined by DFT calculation. The alkyne first coordinates to the Cu(I) species, forming an acetylide (**5**). One of the ligands of complex **5** is then replaced with an azide. The N^1 of this azide coordinates to the copper atom, forming intermediate **6**. This intermediate formed an unusual six-membered copper(III)metallacycle (**7**) through nucleophilic attack of the azide to the carbon atom. The five-membered ring then forms, followed by releasing the 1,4-product. The catalyst was regenerated as shown in Scheme 2.

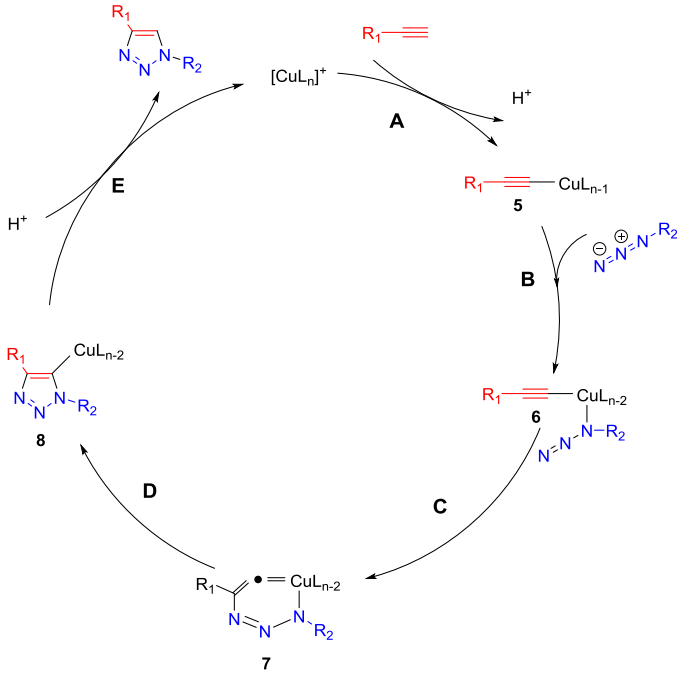

Scheme 2: Proposed reaction mechanism by Fokin *et al.* [9] **The [3+2] cycloaddition between an alkyne and azide in the presence of a copper catalyst.**

In the reaction described above the alkyne can be substituted for a $\lambda^3\sigma^3$-phosphorus. A phosphazene **9** was formed (Scheme 3 reaction A, Staudinger reaction).[4] Using a phosphaalkyne the [3+2] cycloaddition reaction occurred selectively, yielding exclusively the 1,4-product (Scheme 3 reaction B). An advantage of using a phosphaalkyne instead of an alkyne is that no catalyst was needed to obtain a 1,4-product, likely due to the slightly polarized P≡C bond.[4] Another advantage is that these reactions occur quantitatively.[4]

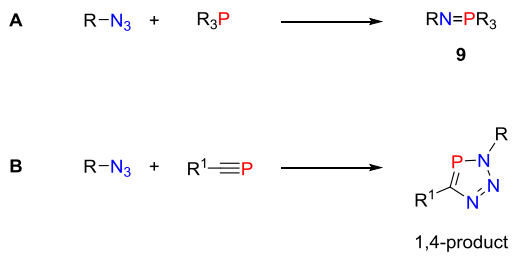

Scheme 3: A reaction between an azide and a classical phosphorus, which gave phosphazene 9 (A). A selective [3+2] cycloaddition between the azide and low-coordinate phosphaalkyne, which gave a selective 1,4-product (B).[4]

Scheme 4 shows the reaction mechanism of this selective [3+2] cycloaddition, including resonance structures of the azide. The P≡C bond undergoes nucleophilic attack from the azide (N^3), and an electrophilic attack occurs of the carbon atom to the N^1 of the azide. This gives the 1,4-product.

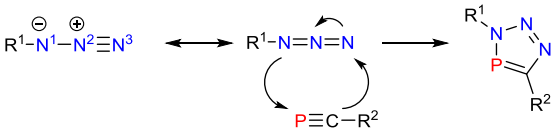

Scheme 4: Reaction mechanism for the selective synthesis of the 3*H*-1,2,3,4-triazaphosphole derivative.

1.4 Properties of 3*H*-1,2,3,4-triazaphosphole derivatives

The 3*H*-1,2,3,4-triazaphosphole derivatives belong to the class of the low-coordinate phosphorus compounds. Their properties are less investigated than the once of phosphines. For example, it is difficult to give a detailed explanation about the steric properties of 3*H*-1,2,3,4-triazaphosphole derivatives, since only a few of them have been characterized crystallographically.[4] These molecular structures show that the 3*H*-1,2,3,4-triazaphosphole is planar. The N-P-C angle is close to 90°, which is representative for these species.[4] The angle from other aromatic compounds containing a phosphorus atom is clearly different. For example, six-membered phosphorus heterocycles (compound **2**) have a C-P-C angle of around 100°.[10]

The 3*H*-1,2,3,4-triazaphosphole derivatives have a conjugated π-system.[11] The phosphorus atom in the ring has high π-density due to the N-C=P ↔ N^+=C-P^- conjugation.[11] One example that demonstrates the electronic properties of triazaphospholes is presented in Figure 3.[12] Here, the cyclic voltammogram spectra of triazaphosphole **10A** and its analogue **10B**, a 1*H*-1,2,3-triazole, were presented. [12] It can be derived that compound **10A** is easier to oxidize than compound **10B** (spectrum A), which is due to the electron-rich properties of compound **10A**. For reduction reactions, compound **10A** is more difficult to reduce (spectrum B), because the LUMO of compound **10A** is higher in energy than the LUMO of compound **10B**. This can also be explained by the presence of an electron-rich heterocycle.[12] Both cyclic voltammograms show that the phosphorus atom in the five-membered ring has an influence on both the oxidation and reduction reaction.

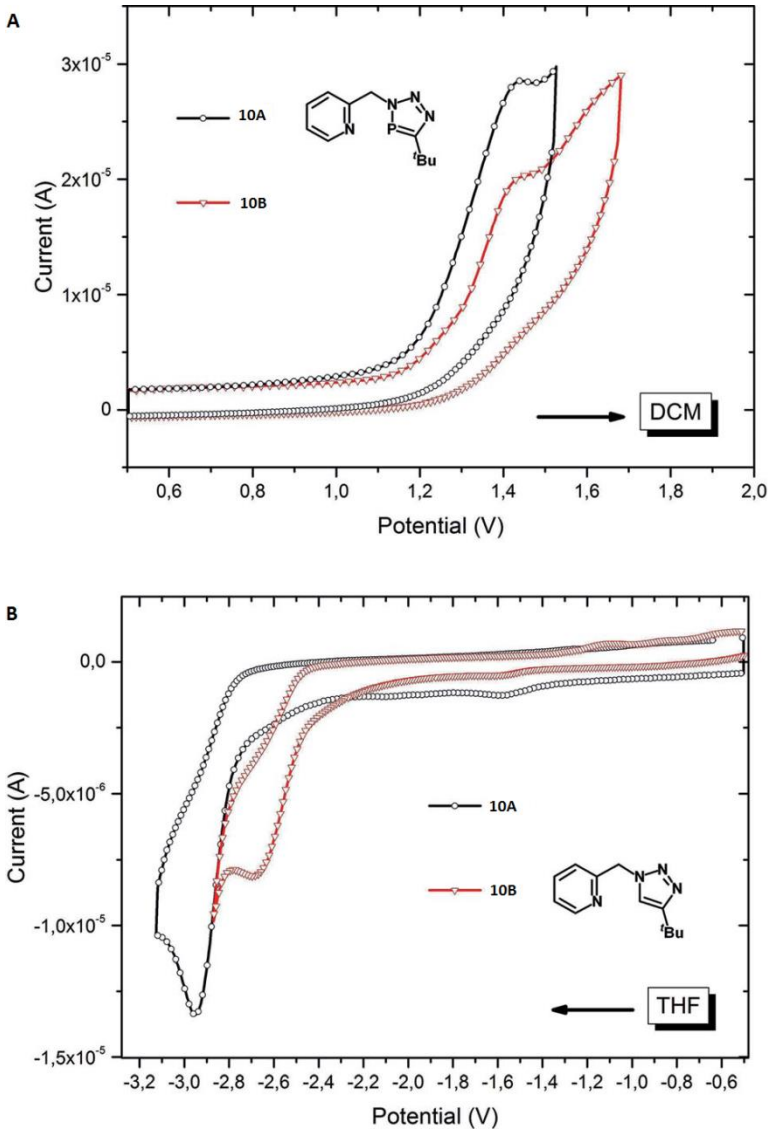

Figure 3: Cyclic voltammetrograms of compounds 10A and 10B. Both compounds have been oxidized (A) and reduced (B).[4,12]

1.5 Coordination of 3*H*-1,2,3,4-triazaphosphole derivatives to transition metals

Derivatives of compound **4** have several coordination sites. Figure 4 shows that the phosphorus and the N^1 and N^2 atoms can coordinate to a metal center.[4] The lone pair of N^3 is embedded into the π-system and therefore cannot coordinate.[4]

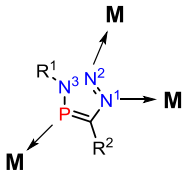

Figure 4: Possible coordination modes of a 3*H*-1,2,3,4-triazaphosphole derivative.[4]

The coordination chemistry of these species is little explored. However, so far no complexes with mono-coordination were reported.[4]

1.6 Examples of 3*H*-1,2,3,4-triazaphosphole derivatives in coordination chemistry

3*H*-1,2,3,4-triazaphosphole are synthesized by using phosphaalkynes and azides as starting materials (Scheme 5). Unfortunately, the variety of phosphaalkynes is limited. Due to poor stability, decomposition occurs.[4] Nevertheless, several different 3*H*-1,2,3,4-triazaphosphole derivatives based on different azides have been synthesized in our group. For the phosphaalkyne in these examples, compounds **13** and **14** were used.

Scheme 5 shows the synthesis of four different 3*H*-1,2,3,4-triazaphospholes. Compounds **15A** and **15B** both have a directly attached conjugated π-electron system.[13] For compound **10A** and **10B** the conjugated π-electron system is interrupted by the methylene bridge.[12] All compounds were analyzed by $^{31}P\{^1H\}$ NMR spectroscopy.[12,13] The signals were found in the range of δ = 160 - 220 ppm, which is typical for 3*H*-1,2,3,4-triazaphosphole derivatives.[4]

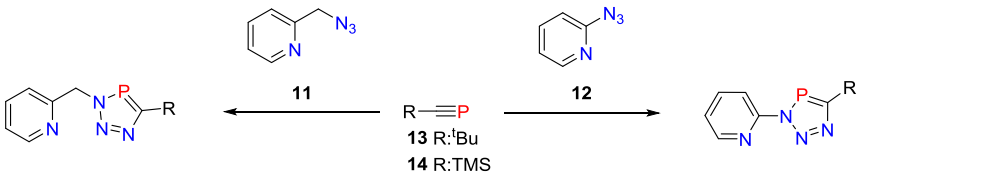

Scheme 5: Overview for the synthesis of several different 3*H*-1,2,3,4-triazaphospholes.[12, 13]

The chelating properties of compounds **10A**, **B** and **15A** were investigated.[12,13] As shown in Figure 4, several different coordination modes are possible. For ligands **10A** and **10B**, complexation with $[Re(CO)_5Br]$ occurred (Scheme 6).[12] X-ray analysis showed that coordination occurred through the N^2 atom of the 3*H*-1,2,3,4-triazaphosphole and the N atom of the pyridine. This coordination mode occurs for both R = TMS or ^{t}Bu. The N^2 is the least nucleophilic nitrogen atom in the 3*H*-1,2,3,4-triazaphosphole.[4] This has never been observed before, but can be explained due to chelating effects. Furthermore, these complexes were analyzed by $^{31}P\{^1H\}$ NMR spectroscopy. In both cases, a downfield shift occurs relative to the free ligand (Scheme 6).

The directly attached conjugated ligand also undergoes complexation with the metal precursor $[Re(CO)_5Br]$.[13] X-ray analysis again showed a coordination by the N^2 of the 3*H*-1,2,3,4-triazaphosphole and the N atom of the pyridine. $^{31}P\{^1H\}$ NMR spectroscopy showed also a downfield in the spectrum compared with the free ligand (Scheme 5 and 6).

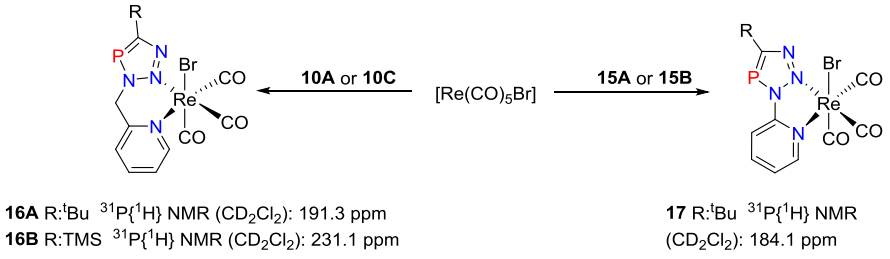

Scheme 6: Coordination of ligands 10A, 10B, 15A and 15B with $[Re(CO)_5Br]$.[12,13]

Species which coordinate via the N^1 are also reported by Jones *et al.*[14] They synthesized a dimeric cationic complex, where the Ag(I) atom coordinates to the two N^1 atoms of the 3*H*-1,2,3,4-triazaphosphole ligand, as shown in Figure 5.[14]

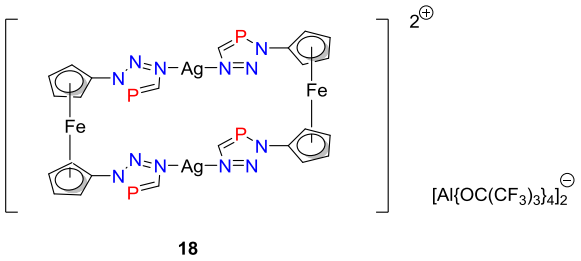

18

Figure 5: Structural formula of complex 18.[14]

Further, the coordination via the phosphorus atom was also reported.[15] Jones *et al*. synthesized ligand **19**, which was used for complexation reactions.[15] Two equivalents of [Pt(norbornene)$_3$] were used for the synthesize of complex **20**, which is an unusual bimetallic species. Three phosphorus atoms coordinate to one Pt(0) atom, while the other Pt(0) atom coordinates to two phosphorus atoms and to the norbornene molecule via a η^2-interaction. (Scheme 7). This shows that the ligand acts as a tripodal P_3 ligand that coordinates via the phosphorus atoms to the Pt(0). Remarkably, this is the only known complex where coordination of the 3*H*-1,2,3,4-triazaphosphole occurs over the phosphorus atoms.

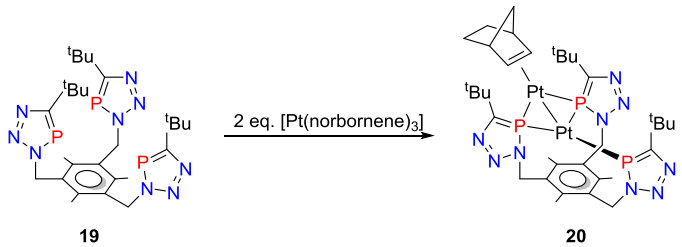

19 **20**

Scheme 7: Reaction of ligand 19 with two equivalents of [Pt(norbornene)$_3$].[15]

1.7 Applications of 3*H*-1,2,3,4-triazaphosphole derivatives

In the past, these species were investigated out of curiosity, but it is now known that their characteristic properties can be used in fields such as homogeneous catalysis[16] or (luminescent) molecular materials.[4]

Their π-conjugated systems are very interesting for organic light emitting diodes.[4] Compounds **15A-C** and **21** were used for measuring their excitation and emission (Figure 6).[13] Compounds **15A** and **15B** both contain a conjugated π-system, where only the R group varies. Compound **15B** differs from **15C** only in that a phosphorus atom is substituted for a carbon atom. This compound was used as a reference. Compound **21** was also used as a reference. Here, the conjugated π-system was interrupted by the methylene bridge.

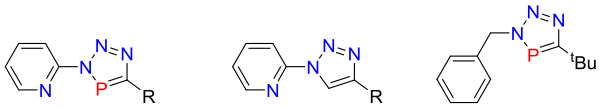

15A R=^{t}Bu
15B R=TMS

15C R=^{t}Bu

21

Figure 6: Compounds 10A, B, C and 21.[13]

The emission spectra were measured for compound **15A** (λ = 370 nm) and **15B** (λ = 334 nm).[13] The R group influences the position of the emission maximum, which might be explained by the electron withdrawing TMS group in compound **15B**.[13] Their analogue, compound **15C**, showed no emission at all.[13] This shows that the presence of the phosphorus atom in the 5-membered ring influences the photophysical properties of the molecule.[13] No emission was obtained for compound **21**, which indicated that a conjugated system was needed.[13]

2. Aim of the project

The goal of this project is to synthesize a new 3*H*-1,2,3,4-triazaphosphole ligand to investigate its bidentate properties in coordination chemistry. To achieve this goal, two different pathways will be used.

Part I

As mentioned in the introduction, few stable phosphaalkynes are known. Therefore, a new diphosphaalkyne **22** will be synthesized. The phosphaalkyne functional groups are connected by an adamantane backbone (Scheme 8). This backbone is rigid and bulky, which might result in a stable molecule. After this molecule is synthesized, it will be used in [3+2] cycloaddition reactions with different azides. The resulting 3*H*-1,2,3,4-triazaphospholes will be characterized and used as ligands in coordination chemistry. (Scheme 8 compound **24**).

Part II

In the second part, the process is reversed. Instead of synthesizing the diphosphaalkyne, the diazide **23** will be synthesized. This compound will be used in [3+2] cycloaddition with different phosphaalkynes (Scheme 8). However, few phosphaalkynes are stable. Therefore, fewer 3*H*-1,2,3,4-triazaphospholes (**25**) will be synthesized than for part I. Here also, the coordination chemistry will be investigated.

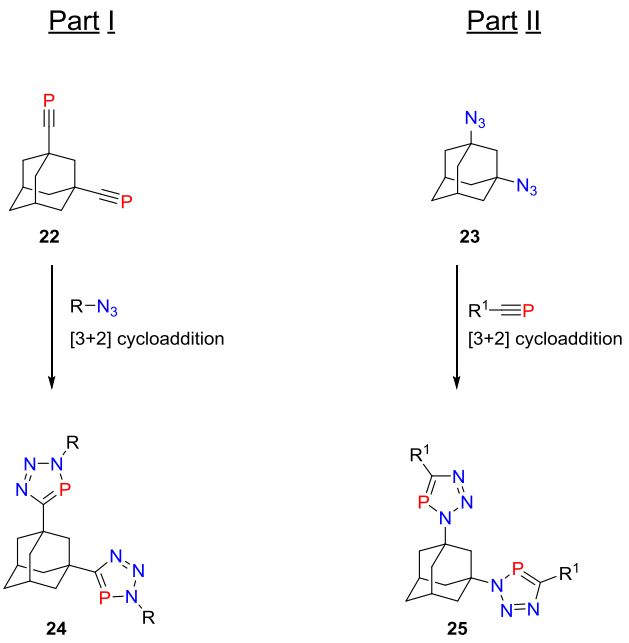

Scheme 8: An overview of the project. Part I shows the synthesis of diphosphaalkyne 22. It was used in [3+2] cycloaddition reactions with several different azides. Part 2 shows that the diazide 23 was synthesized. This compound was used in [3+2] cycloaddition reaction with several different phosphaalkynes. In the synthesized 3*H*-1,2,3,4-triazaphosphole (24 and 25), the nitrogen and phosphorus atoms are different orientated in the 5-membered ring.

As mentioned before, we are interested in the behavior of these molecules in coordination chemistry, particularly the bidentate properties of these ligands. Several different late transition metals will be used to investigate this. Scheme 9 shows a schematic representation of how coordination might occur when adding a ligand to the metal precursor. In the first complex (**A**) that might be formed, coordination occurs to both 3*H*-1,2,3,4-triazaphosphole arms via the N or P atom.

The second complex (**B**) shows a bimetallic species. Here, two different atoms coordinate to each arm. These possibilities will be investigated.

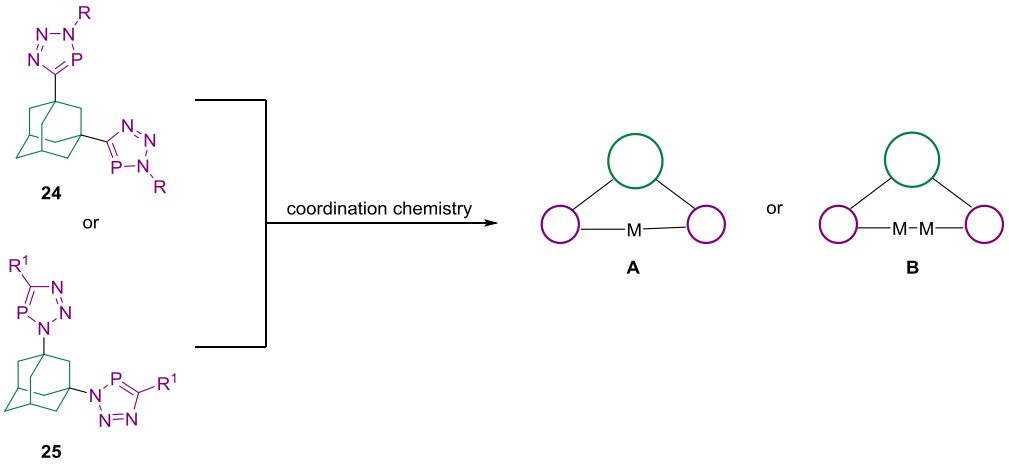

Scheme 9: Schematic representation of the coordination of compound 24 and 25 to a metal. In case A, the metal coordinates to both arms via the P or N atom. In case B, a bimetallic species is formed.

3. Results and discussion

3.1.1 Description of part I

The synthesis of compound **22** is described by Veeck *et al.*[17] Unfortunately, the synthetic pathway is poorly reported. Some parameters, like temperature, reaction time, are missing for the reactions. Regitz *et al.* reported the reaction conditions for the synthesis of the monophosphaalkyne.[18] Therefore a combination of both described procedures was used for the synthesis of compound **22**.

The retro-synthesis of compound **22** described by Veeck *et al.* is presented in Scheme 10.[17] The first step in this retro-synthesis is the conversion of the carboxylic acid **28** to the carboxylic acid chloride **27**. This is followed by the synthesis to the phosphaylidene **26**, which is then converted to phosphaalkyne **22**.

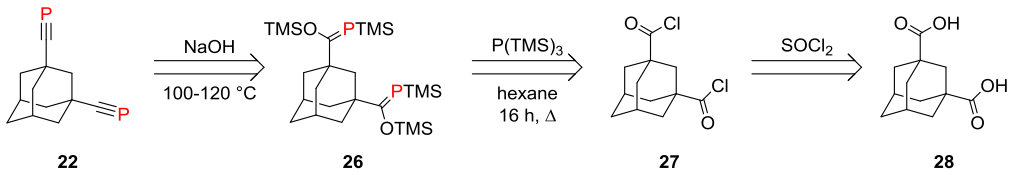

Scheme 10: Retro-synthesis described by Veeck *et al.* for the synthesis of the diphosphaalkyne 22.[17]

3.1.2 Synthesis of the phospaalkyne 26

The first step was the conversion of compound **28** to compound **27** (Scheme 11). This reaction was performed with thionyl chloride as reactant and solvent. A catalytic amount of DMF was added to enhance the solubility of carboxylic acid **28**. After 4 h of refluxing, no HCl and SO_2 gas occurred, which indicated that the reaction was complete. Analysis of compound **27** was performed by IR spectroscopy, which showed no characteristic band for the –COOH functional group. Furthermore, an esterification reaction was performed. A small amount of compound **27** was dissolved in dry EtOH. The excess of EtOH was removed and the sample was measured by ^{1}H NMR spectroscopy. The signals showed that an ester was formed and no starting material or mono substitution of the carboxylic acid was obtained.

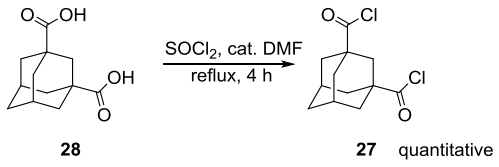

Scheme 11: Syntheses of compound 27.[17, 19]

For the synthesis of the phosphaylidene **26**, several different reaction conditions were used. Since the described method by Veeck *et al.*[17] was not complete, a different method was used i.e. the one of Regitz *et al.*[18] Here, pentane was used as the solvent. The reaction conditions were described in Scheme 12.

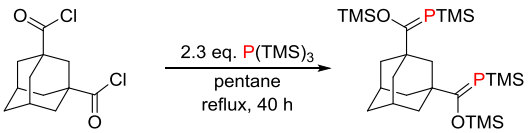

27 26

Scheme 12: Synthesis of compound 26.

Compound **27** was not soluble in pentane, so the mixture was refluxed. Monitoring the reaction using $^{31}P\{^{1}H\}$ NMR spectroscopy showed a chemical shift of δ = 124.9 ppm after 8 h refluxing (Figure 7 spectrum A). According to Veeck *et al.,* this signal indicated that the product was formed.[17] However, the signal at δ = -250 ppm indicated that there is still $P(TMS)_3$ present in the mixture. The intensity of this signal is high, indicating that the reaction was still proceeding. Other signals in the $^{31}P\{^{1}H\}$ NMR spectroscopy could not be explained.

Refluxing the mixture for another 16 h showed an increase of the product signal (Figure 7 spectrum B). Most other signals vanished, which could indicate that they were intermediates of the product. The reaction was continued until no decrease of the $P(TMS)_3$ signal was observed (Figure 7 line C). Purification of the product was performed by removing $P(TMS)_3$ by vacuum distillation. Recrystallization attempts did not result in pure product (Figure 7 line D).

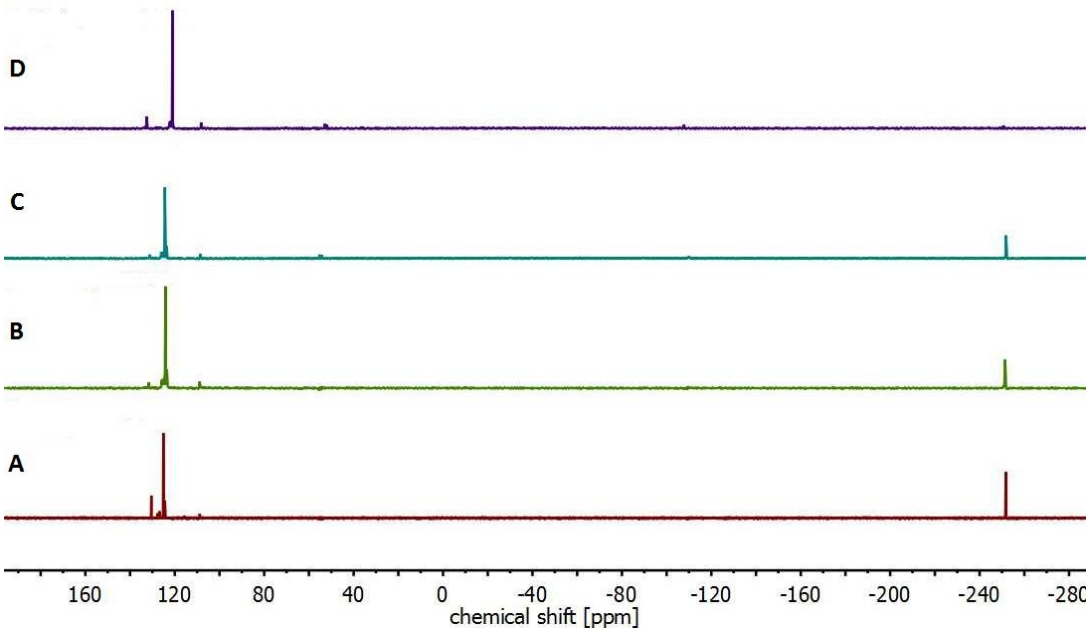

Figure 7: An overview of the $^{31}P\{^{1}H\}$ NMR spectra for the synthesis of compound 26 as described in Scheme 12. First, the reaction mixture was refluxed for 8 h (spectrum A). The reaction time was increased for 16 h (spectrum B) and then again increased for another 16 h (spectrum C). Vacuum distillation and recrystallization attempts gave spectrum D.

The synthesis of compound **26** was repeated on larger scale. Since this reaction needed elevated temperatures, the reaction was performed in a pressure tube. First, the mixture was heated for 2 days at T = 50 °C. $^{31}P\{^{1}H\}$ NMR spectroscopy revealed several signals, including one of the starting material $P(TMS)_3$ (Figure 8 spectrum A). This signal had a high intensity, whereas the signal of the product (at δ = 124.9 ppm) was weak. This showed that the reaction was not successful. A possible explanation could be that the $P(TMS)_3$ could not react with the acid chloride, because the acid chloride did not entirely dissolve in pentane. To improve solubility, DCM was added. Heating the

mixture at T = 50 °C for 16 h gave no increase of the product signal (Figure 8 spectrum B). Increasing the reaction time for 2 days gave spectrum C (Figure 8). Unfortunately, the intensity of the signal showed no increase. The $^{31}P\{^{1}H\}$ NMR spectra of B and C were comparable.

More harsh reaction conditions were used by increasing the temperature to T = 80 °C for 48 h. The $^{31}P\{^{1}H\}$ NMR spectrum showed that the chemical shift of the product (around δ = 124.9 ppm) vanished. This might be explained by the reactivity of the C=P bond at elevated temperatures. Due to the higher reaction temperature, the C=P might react further to form a more stable product. This could also explain the new signals at δ = 197 ppm. This chemical shift was not visible in spectra A, B or C.

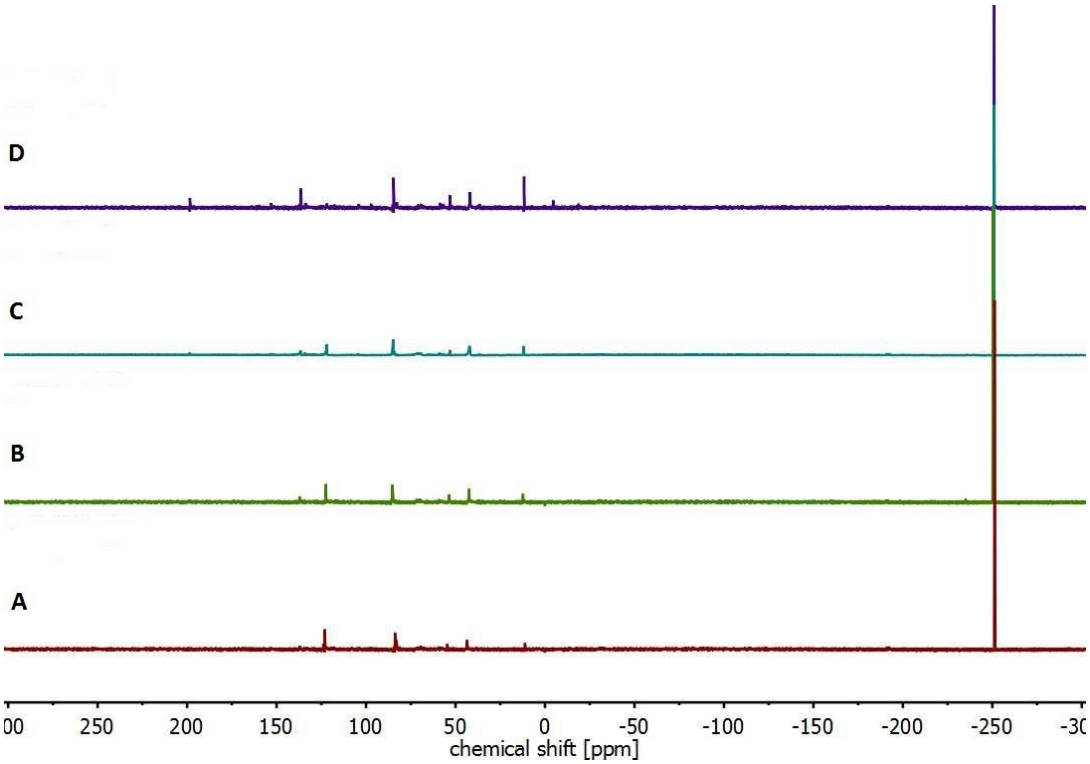

Figure 8: An overview of the $^{31}P\{^{1}H\}$ NMR spectra for the synthesis of compound 26. The reaction was carried out in a pressure tube. The mixture was heated at T = 50 °C for 2 days (spectrum A). After adding DCM to the mixture the reaction time was increased for 16 h (spectrum B). Increasing the reaction time to 2 days gave spectrum C. Increasing the temperature to 80 °C for 2 days gave spectrum D.

Both reactions showed problems with the solubility of compound **27** in pentane. Even when the reaction mixture was heated, not all the starting material dissolved. Since Veeck *et al.* used hexane as solvent, the pentane was substituted for hexane.[17] Also, a slightly bigger excess of the $P(TMS)_3$ was used, as presented in Scheme 13.

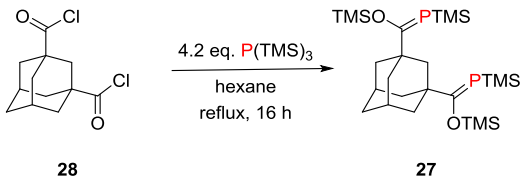

28 **27**

Scheme 13: Synthesis of compound 27. In contrast as with the previous synthesis, hexane was used as the solvent instead of pentane.

After refluxing the mixture for 16 h, precipitation formed in the reaction mixture. The precipitate was separated from the liquid. Both fractions were analyzed by $^{31}P\{^{1}H\}$ NMR spectroscopy and had comparable spectra (Figure 9). Both fractions contain the starting material (δ = -250 ppm) and product (δ = 121 ppm).

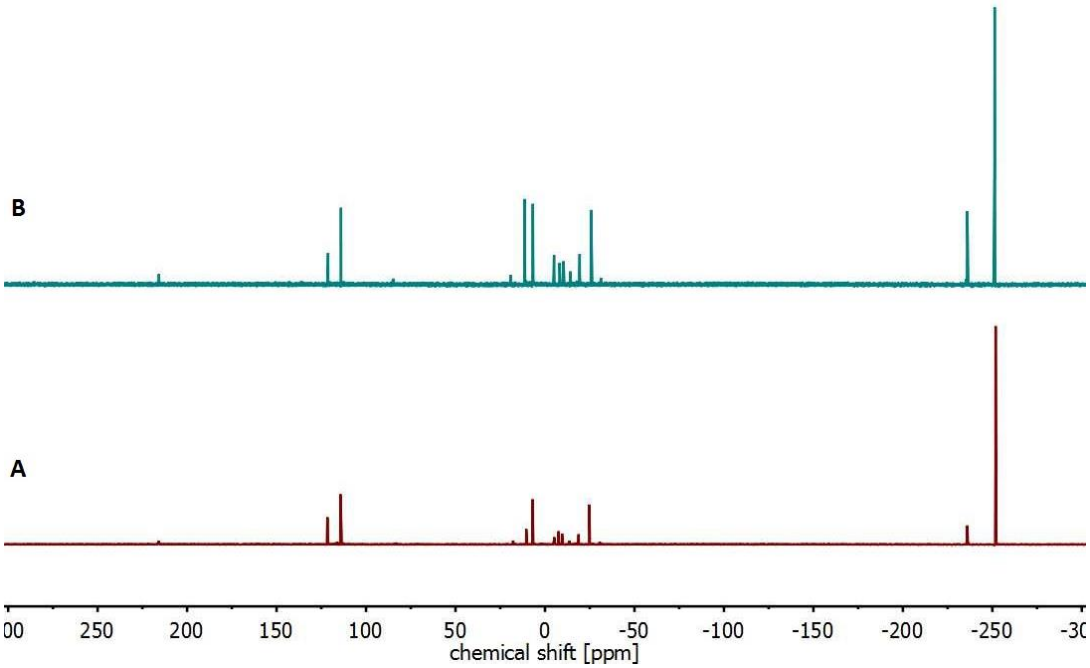

Figure 9: An overview of the $^{31}P\{^{1}H\}$ NMR spectra obtained for the synthesis of compound 27 as described in Scheme 13. Spectrum A is from the liquid layer and spectrum B from the precipitate.

$^{31}P\{^{1}H\}$ NMR spectroscopy showed that the starting material remained unreacted after several hours of heating (Figure 8 and 9). The phosphorus atom in the $P(TMS)_3$ is surrounded by bulky TMS groups. This causes steric hindrance around the phosphorus atom, which may prevent nucleophilic attack on the carbon atom of compound **27**.[20] Therefore, the starting material remained unreacted in the reaction mixture.

Due to the sterically bulky groups surrounding the phosphorus atom in $P(TMS)_3$, a different approach was used. The starting material was substituted by $LiP(TMS)_2{\cdot}2$ THF. The phosphorus atom in this compound has one fewer TMS group and is therefore less bulky. Furthermore, the solvent was changed to THF to avoid solubility problems.

In the first approach a solution of THF and $LiP(TMS)_2{\cdot}2$ THF was added dropwise to a solution of the acid chloride in THF. The flask was covered in aluminum foil and stirred for 48 h at room temperature (Scheme 14).

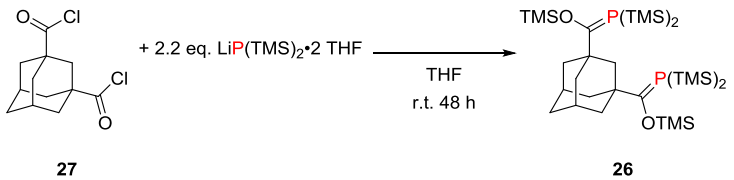

27 **26**

Scheme 14: Synthesis of compound 26. For the starting material $LiP(TMS)_2{\cdot}2$ THF was used with THF as the solvent. The reaction was stirred for 48 h at r.t.

$^{31}P\{^{1}H\}$ NMR spectroscopy revealed several signals (Figure 10 spectrum A). None of them had a chemical shift which corresponded to the product. The reaction was repeated, but the reaction time was decreased to 16 h. Furthermore, the solvent THF was dried over NaK to make sure water was excluded from the reaction mixture. Water can react with the reactive P=C bond, which might explain the amount of signals in $^{31}P\{^{1}H\}$ NMR spectra.

After the reaction, the solvent was removed in vacuo and the residue was analyzed. However, it was only partly soluble in deuterated benzene. The $^{31}P\{^{1}H\}$ NMR spectra obtained in Figure 10 gave no clear picture of the products that were formed (spectrum B). According to Veeck *et al.,* the product should be soluble in deuterated benzene and therefore the product was not formed during these reaction conditions.

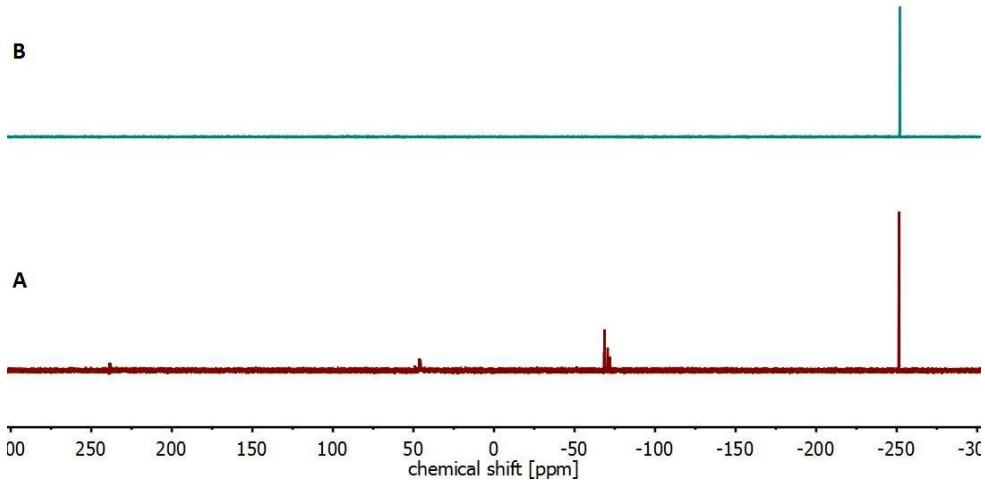

Figure 10: Overview of $^{31}P\{^{1}H\}$ NMR spectra when using $LiP(TMS)_2 \cdot 2$ THF as the starting material. Spectrum A was obtained after a reaction time of 48 h. Spectrum B was obtained when the THF was dried over NaK and the reaction time was decreased to 16 h.

Compound **27** could not be converted to compound **26** using the reaction conditions described above. The signals that do not appear in spectrum B (compared with spectrum A) might be due to the shorter reaction time.

3.1.3 Synthesis of phosphaalkyne 22

The reaction described in Scheme 12 showed the formation of product **26**. Since it could not be further purified, the next reaction was performed using this mixture. This reaction was monitored using $^{31}P\{^{1}H\}$ NMR spectroscopy. Figure 11 shows an overview of the zoomed-in spectra; the entire spectra may be found in the appendix. For this reaction, an excess of NaOH was used, and DME was used as solvent (Scheme 15).

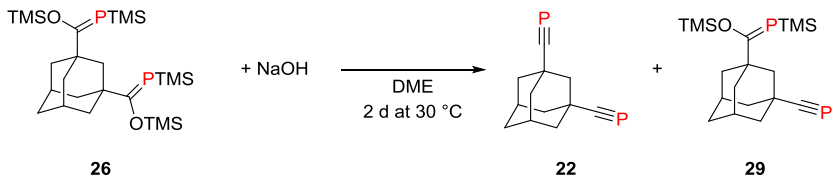

Scheme 15: Synthesis of compound 22.

The mixture was initially stirred for 16 h at room temperature. No product was obtained (spectrum A); according to Veeck *et al.,* the phosphorus atoms of the product gave a signal at δ = -66.9 ppm (in C_6D_6).[17] Heating to T = 30 °C for 2 days showed some product formation (spectrum B). Increasing the reaction time for 5 days gave spectrum C. Increasing the time for another 2 days gave spectrum D.

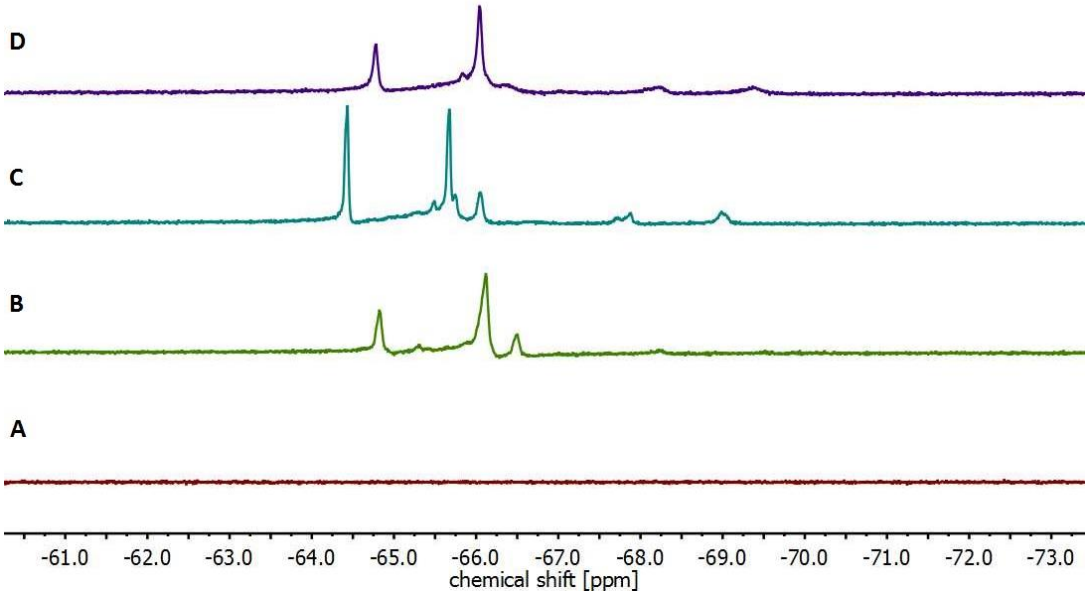

Figure 11: Overview of the obtained $^{31}P\{^1H\}$ NMR spectra for the synthesis of compound 22 as described in Scheme 15. When the mixture was stirred at r.t. for 16 h, no product was obtained (spectrum A). Increasing the temperature and reaction time to T = 30 °C for 2 days gave spectrum B. The reaction time was again increased for 5 days (spectrum C) and later for another 2 days (spectrum D).

Since some product formation was observed, an attempt to purify the compound was performed. Removal of the DME was performed by vacuum distillation, which was not successful. Attempts to recrystallize or column chromatography failed as well.

A second attempt to synthesize compound **22** employed harsher reaction conditions. No solvent was used and the mixture was heated to T = 125 °C for 2 h (Scheme 16).

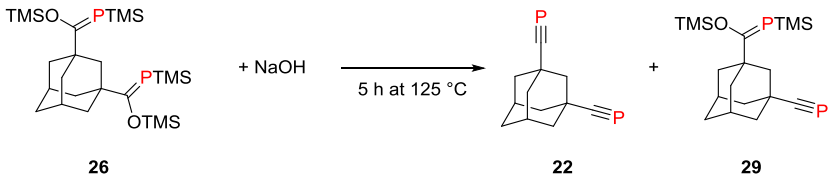

Scheme 16: Synthesis of compound 22. No solvent was used and the temperature was increase to T = 125 °C. The reaction time was decreased to 5 h.

Besides product formation, some side products were observed (Figure 12 spectrum A). Most of the starting material had not reacted. Increasing the reaction time for another 3 h gave the spectrum shown in Figure 12 (spectrum B). Here the chemical shift at δ = -66 ppm vanished. It might be that the product is unstable and therefore decomposed when increasing the reaction time at high temperature.

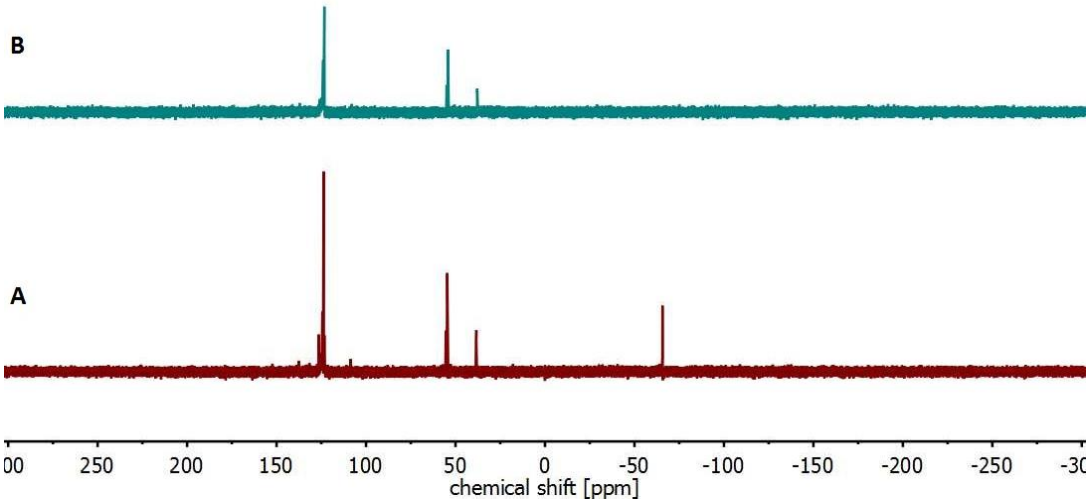

Figure 12: Spectrum A shows product formation at δ = -66 ppm. This $^{31}P\{^{1}H\}$ NMR spectrum was obtained after 2 h of heating the reaction mixture at T = 125 °C. Increasing the reaction time for another 3 h gave spectrum B.

The first part of this project was to synthesize compound **22**. The first step in this reaction sequence was the synthesis of the carboxylic acid chloride **27**. This compound was obtained in high yield. When performing the synthesis of phosphaylidene **26**, several different reactants and conditions were used. Only one of these reactions gave the desired product. The reaction conditions using $P(TMS)_3$ as the starting material can be compared with each other. The reaction mixture that was obtained after the synthesis at high temperature (Figure 8 and 9) showed no resonance or only low-intensity ones in $^{31}P\{^{1}H\}$ NMR spectroscopy. The product was obtained (Scheme 12 Figure 7) when lower temperatures were used. This might indicate that compound **26** is unstable at high temperatures. This might also be the case for compound **22**. Figure 12 shows clearly that when the reaction time was increased (at T = 125 °C), the signal at δ = – 66 ppm vanished.

Due to these results, the project was changed. Instead of synthesizing the diphosphaalkyne **22**, the diazide **23** was synthesized. This will be discussed in the next section.

3.2.1 Description of part 2

3.2.2 Synthesis of diazide 23

The project was switched to the synthesis of the diazide **23**. After obtaining this compound, it was used for [3+2] cycloaddition reactions. Here, several different phosphaalkynes were used. The synthesis of these different 3*H*-1,2,3,4-triazaphospholes will be discussed in section 3.2.3 until 3.2.5.

First, the synthesis of the diazide **23** was performed according to the method described by Davis and Nissan.[21] In this reaction, the $SnCl_4$ acts as a Lewis acid forming a stable tertiary carbocation on the adamantane ring. Nucleophilic attack of the TMS-N_3 to the adamantane afforded the product in a yield of 89 %. Scheme 17 shows the reaction conditions.

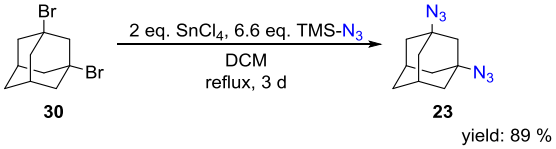

Scheme 17: Synthesis of compound 23.[21]

3.2.3 Synthesis of ^{t}BuTAP 32

The diazide was used in a [3+2] cycloaddition with phosphaalkyne **31** (Scheme 18). Phosphaalkyne **31** is unstable and highly flammable, so an excess of a THF and compound **31** solution were transferred via trap-to-trap condensation. Removal of the excess occurred through another trap-to-trap condensation, which gave a white solid. Analysis by $^{31}P\{^{1}H\}$ NMR spectroscopy showed a chemical shift of δ = 163.08 ppm (Figure 13). Only one singlet was obtained, because the molecule contained an inner mirror image.

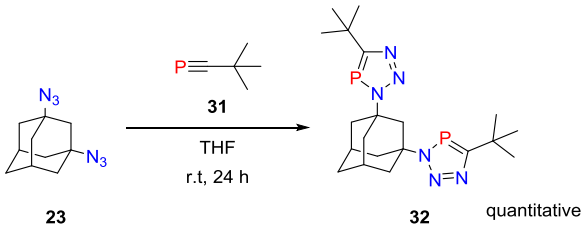

Scheme 18: [3+2] Cycloaddition between compounds 23 and 31.

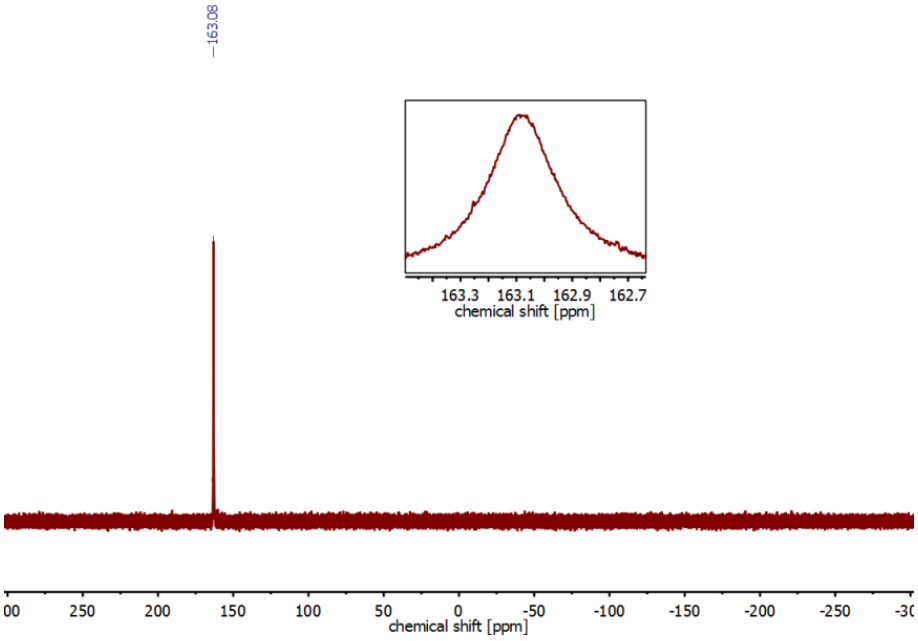

Figure 13: $^{31}P\{^{1}H\}$ NMR spectrum of compound 32 measured in CD_2Cl_2.

To exclude the possibility that only one azide group had reacted, mass spectrometry was performed. The protonated mono 3*H*-1,2,3,4-triazaphosphole **33** has a m/z value of 319.1795, which was not observed in the spectrum. The m/z value from the obtained spectrum matched with the calculated m/z distribution of compound **32** (Figure 14).

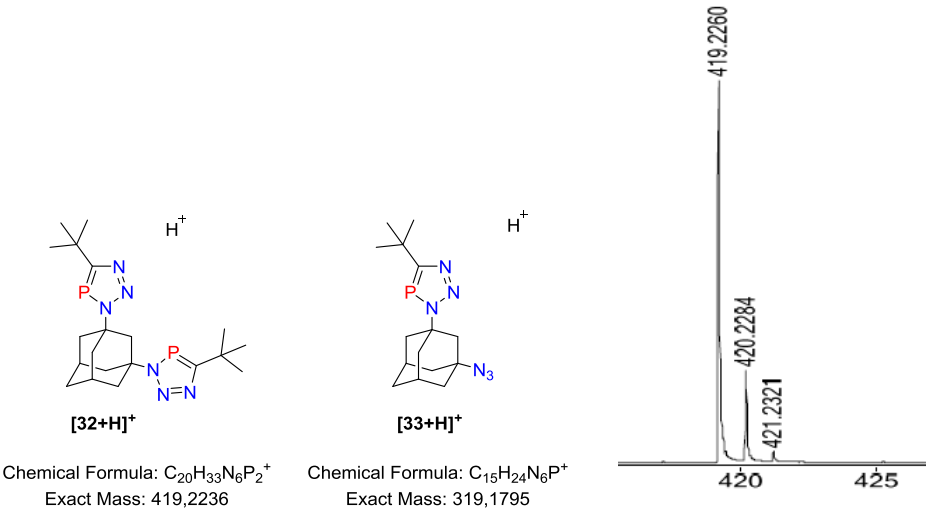

Figure 14: Calculated m/z value for the protonated compounds 32 and 33 (left). A zoomed-in section of the obtained mass spectrum is presented (right).

Recrystallization from a hot hexane solution yielded single crystals which were of adequate quality for X-ray diffraction measurements. Figure 15 shows the measured molecular structure of compound **32** in the crystal. The P=C bond distances are 1.716 Å and 1.722 Å. These distances lay in between the reported values of a localized double (ca. 1.66 Å) and single (ca. 1.87 Å) bond.[22]

Another interesting distance was that between the two 3*H*-1,2,3,4-triazaphosphole arms. In the solid state, the nitrogen atoms point towards each other. The distance between N(1)-N(3) is 5.287 Å and

the N(2)-N(4) distance is 7.489 Å (Figure 15). For compound **32** to behave as a bidentate ligand, the distances between the nitrogen atoms might be too large to form a complex as presented in Scheme 9 complex A. This ligand might still form a bimetallic species (Scheme 9 complex B), but this depends on which metal is used. When the 'arms' of the ademantane ring are rotated the phosphorus atoms can point towards each other. The distance is around 4 Å, which is smaller than the N(1)-N(3) distance. Therefore it might still act as a bidentate ligand (Scheme 9 complex A and B). The coordination chemistry of this ligand to various metal centers will be discussed in section 3.3.

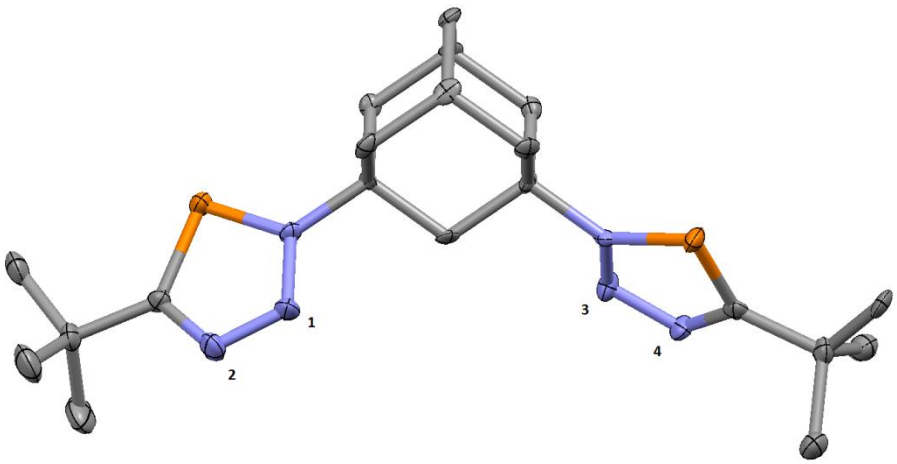

Figure 15: ORTEP plot of the molecular structure of compound 32 in the crystal. Ellipsoids are shown at the 50 % probability level. Hydrogen atoms are omitted for clarity.

3.2.4 Synthesis of TMS-TAP 35

The next reaction was performed between phosphaalkyne **34** and compound **23** (Scheme 19). Just as for the previous [3+2] cycloaddition, a solution of compound **34** in toluene was added to compound **23**. Since the phosphaalkyne **34** is thermally unstable, the reaction was carried out at T = -20 °C for 24 h. Removal of toluene and starting material **34** was performed by evaporation under reduced pressure.

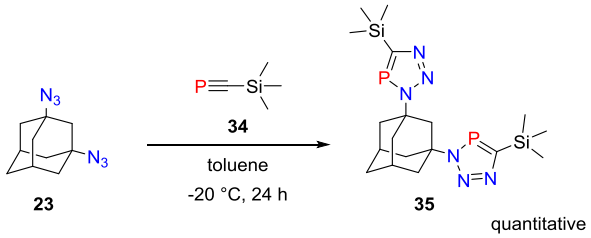

Scheme 19: [3+2] Cycloaddition between compound 23 and 34.

This molecule contained an internal mirror image. Analysis by $^{31}P\{^{1}H\}$ NMR spectroscopy showed only one singlet at δ = 206.21 ppm (Figure 16).

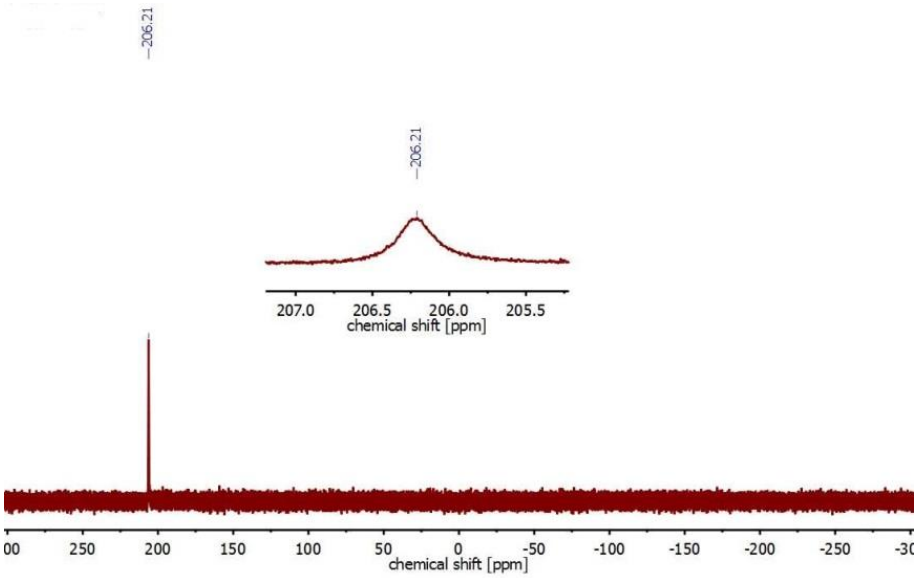

Figure 16: $^{31}P\{^{1}H\}$ NMR spectrum of compound 35 measured in CD_2Cl_2.

Here, mass spectrometry was used to confirm the formation of bis triazaphosphole species **35**. $^{31}P\{^{1}H\}$ NMR spectroscopy cannot distinguish between compound **35** and **36**. Mass spectrometry showed no m/z value corresponding to the protonated mono 3*H*-1,2,3,4-triazaphosphole **[36+H]**$^{+}$. For compound **[35+H]**$^{+}$, the m/z value distribution from the obtained spectrum matches with the calculated m/z value (Figure 17).

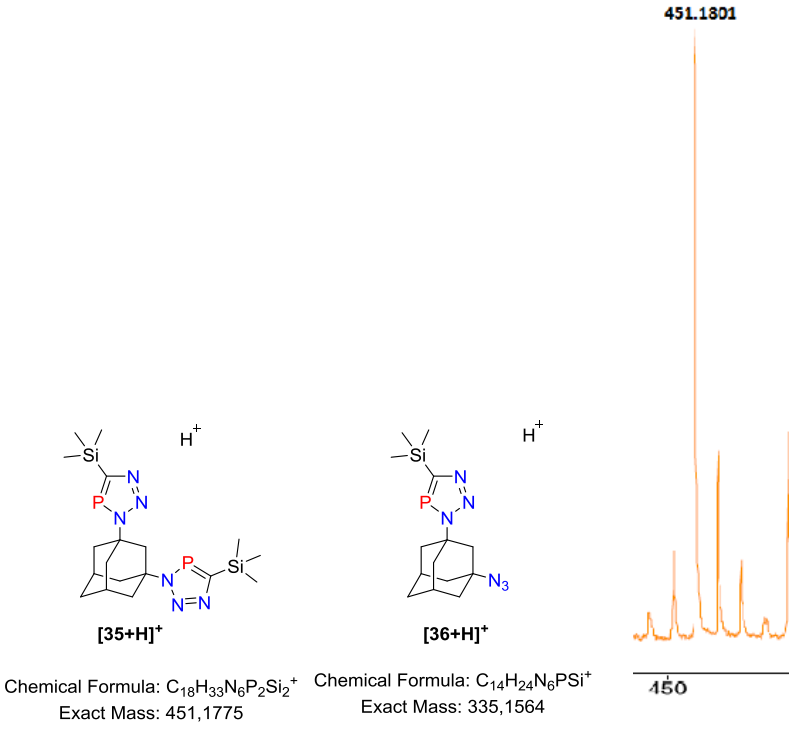

Figure 17: Calculated m/z values for the protonated compounds 35 and 36 (left) and a zoomed-in piece of the obtained mass spectrum (right).

Crystals were obtained from a hot pentane solution. While they were of low quality, their molecular structure could still be proven. Another measurement of a new crystallization attempt will be performed, and thus, this molecular structure will not be discussed in this report.

3.2.5 Synthesis of Mes*-TAP ligand 37

The last [3+2] cycloaddition was performed between compound **23** and phosphaalkyne **36** (Scheme 20). For this reaction, an excess of the diazide **23** was used.

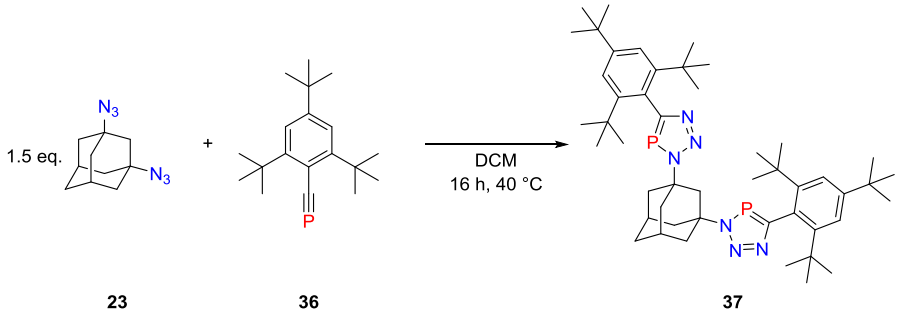

23 **36** **37**

Scheme 20: [3+2] Cycloaddition between compound 23 and 36.

The reaction was followed using $^{31}P\{^{1}H\}$ NMR spectroscopy. The mixture was, as in previous ''click'' reactions, stirred at r.t. for 24 h. $^{31}P\{^{1}H\}$ NMR spectroscopy showed a signal corresponding to the starting material. Heating was necessary due to the bulky tert-butyl groups on the 2, 4, and 6 positions of the aromatic phosphaalkyne **36**. After heating at T = 40 °C for 16 h, two singlets were obtained in $^{31}P\{^{1}H\}$ NMR spectroscopy (Figure 18). The 3*H*-1,2,3,4-triazaphosphole arms cannot rotate freely due to the bulky groups, so the phosphorus atoms have different chemical environments and different chemical shifts. This difference in chemical shift is small, as presented in Figure 18.

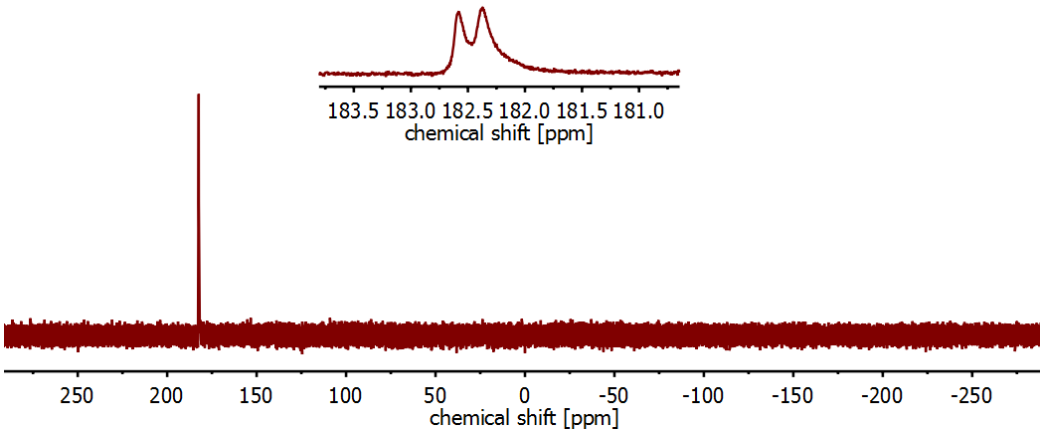

Figure 18: $^{31}P\{^{1}H\}$ NMR spectrum of compound 37 measured in CD_2Cl_2

^{1}H NMR spectroscopy revealed a mixture of signals for two different compounds, since an excess of compound **23** was used. Purification of compound **37** was attempted, but unfortunately all methods have been unsuccessful.

3.3 Coordination chemistry with ^{t}BuTAP 32

The behavior of ligand **32** in coordination chemistry was investigated with different metals. Furthermore, the ratios (in mol) between the metal precursor and ligand were varied.

Attempts in coordination chemistry with Cu(I)

Our group has previously examined the coordination of copper to low-coordinate phosphorus. Several different copper precursors were used, but crystals were only obtained for the $[CuOTf]_2{\cdot}C_6H_6$ and $CuBr{\cdot}SMe_2$ precursors. For the $[CuOTf]_2{\cdot}C_6H_6$ precursor, a 3*H*-1,2,3,4-triazaphosphole derivative was used as ligand.[23] For the $CuBr{\cdot}SMe_2$ precursor, the low-coordinate phosphorus compound **38** was used for complexation. A cluster complex (**39**) was obtained as presented in Scheme 21.[24]

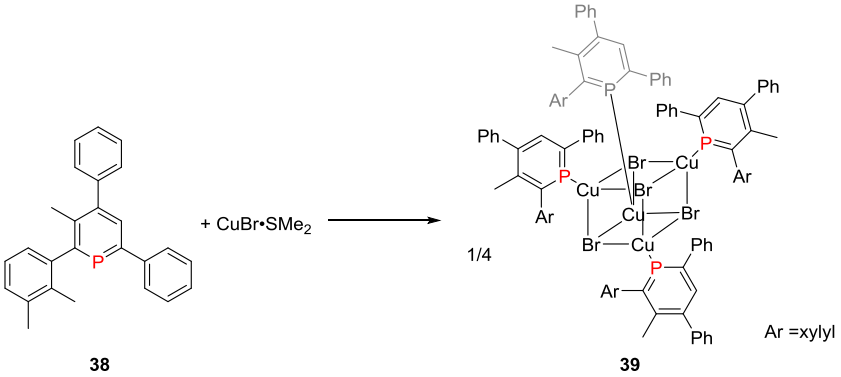

Scheme 21: Synthesis of complex 39.[24]

As discussed in Chapter 1, not much is known about complexes where 3*H*-1,2,3,4-triazaphosphole derivatives are used as ligands. The copper precursors, $[CuOTf]_2{\cdot}C_6H_6$ and $CuBr{\cdot}SMe_2$, are known to coordinate to low-coordinate phosphorus compounds.[23,24] Therefore, these copper precursors were used for complexation with ligand **32**. All coordination attempts were performed in a Y.R. Young tube and analyzed using $^{31}P\{^{1}H\}$ NMR spectroscopy. First, the metal complexation attempts involving the precursor $[CuOTf]_2{\cdot}C_6H_6$ will be discussed.

Figure 19 shows an overview of the obtained $^{31}P\{^{1}H\}$ NMR spectra. These spectra belong to the experiment where a 2:1 ratio of the ligand to metal precursor was used. Here, one metal atom might coordinate to one ligand (Scheme 9 complex A). With this experiment, the bidentate properties of ligand **32** could be investigated. Spectrum B showed only one singlet at δ = 167.5 ppm. This signal is $\Delta\delta$ = 4.4 ppm down shifted compared with the free ligand (Spectrum A). Since $[CuOTf]_2{\cdot}C_6H_6$ was poorly soluble in DCM, the mixture was radiated in an ultrasonic bath for 1 h (Spectrum C). $^{31}P\{^{1}H\}$ NMR spectrum showed no change in chemical shift or additional signals. Heating the mixture for 3 h at T = 60 °C (Spectrum D) showed no change.

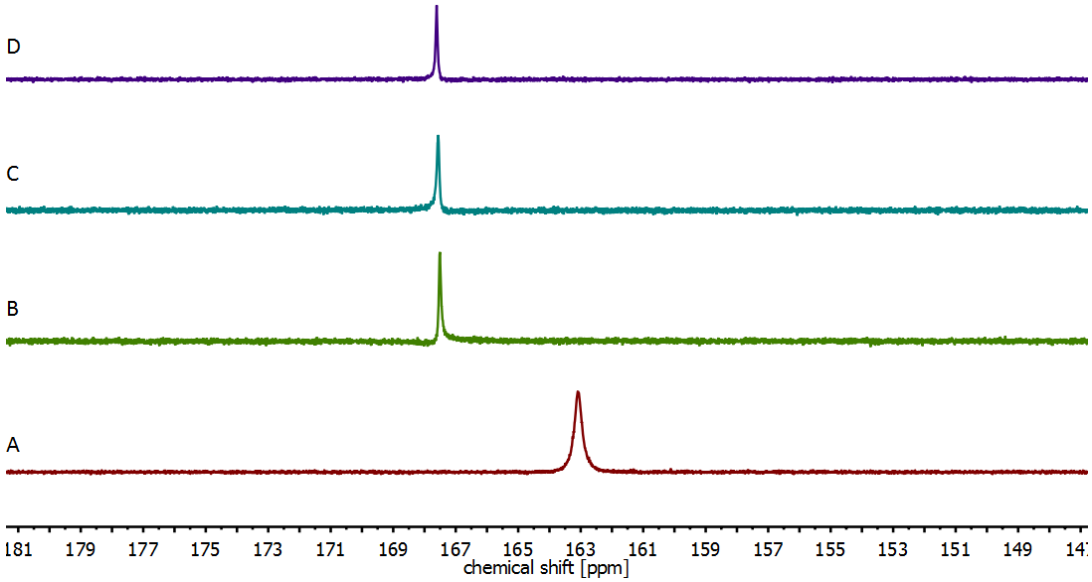

Figure 19: Overview of the obtained $^{31}P\{^{1}H\}$ NMR spectra. These spectra belong to the complexation reaction where the 2:1 ratio of ligand 32:$[CuOTf]_2 \cdot C_6H_6$ was used. Spectrum A belongs to the free ligand. Spectrum B was measured 5 minutes after the copper metal precursor was added at r.t. Radiating the mixture in an ultra-sound bath (spectrum C) gives the same spectrum as (D), but obtained upon heating the mixture for 3 h.

If coordination of the copper atom occurred to only one of the two 3*H*-1,2,3,4-triazaphosphole arms, two signals in $^{31}P\{^{1}H\}$ NMR spectrum should be obtained. There is no symmetry anymore and therefore the two phosphorus atoms have different chemical environments (Scheme 22 complex B). Therefore, no mono coordination from one of the two 3*H*-1,2,3,4-triazaphosphole to the copper atom occurred. If coordination of the two 3*H*-1,2,3,4-triazaphospholes to one copper atom occurred (Scheme 22 complex A), only one singlet would be obtained.

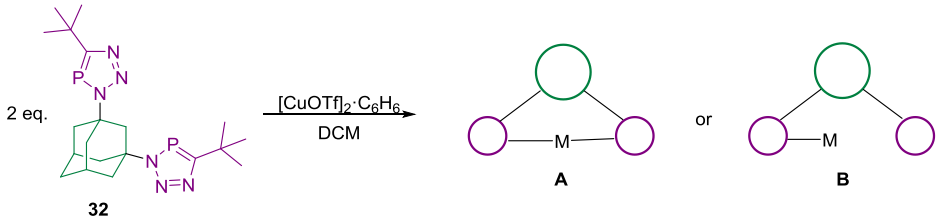

Scheme 22: Schematic representation of the complexation reaction between compound 32 and the copper precursor. In the first case (A), the metal coordinates to both 3*H*-1,2,3,4-triazaphospholes. In the second case (B), the metal coordinates only to one of the two arms, which is according to the spectra in Figure 19 not possible.

The difference in chemical shift between spectra A and B is Δδ = 4.4 ppm. This is a small difference, which might be explained by coordination of the nitrogen atoms of compound **32** to the copper centre. Phosphorus coordination would likely have a more significant chemical shift. The small change in the environment might cause the change in chemical shift. The experiment was repeated with an added standard.

Triphenylphosphine oxide was used as internal standard, because it is assumed to be a weak ligand. The phosphorus atom in this molecule has no free electron pair to coordinate to a metal center. First, the ligand and the triphenylphosphine oxide were added together and measured by $^{31}P\{^{1}H\}$ NMR spectroscopy. Secondly, the ligand and metal precursor were measured again by $^{31}P\{^{1}H\}$ NMR spectroscopy. Triphenylphosphine oxide was then added to the mixture and another measurement

was performed. If the distance between the ligand and triphenylphosphine oxide changed when the metal precursor was present in the sample, then possibly no coordination had occurred. The difference in chemical shift between the ligand and triphenylphosphine oxide was Δδ = 135.7 ppm. For the assumed Cu(I) complex, the difference in chemical shift lies at Δδ = 136.5 ppm. This chemical shift difference is small, and therefore it is possible that the coordination was not successful.

The amount of metal precursor was increased to investigate if this ligand coordinates to the metal precursor. Figure 20 shows an overview of the spectra where a 1:1 mol ratio of the metal precursor: ligand **32** was used. Spectrum B shows a singlet at δ = 168.8 ppm. A downfield shift occurred when comparing spectrum B with A. Heating the mixture at T = 60 °C for 16 h showed a chemical shift of δ = 163.1 ppm (spectrum C). This corresponds to the same chemical shift as from the free ligand.

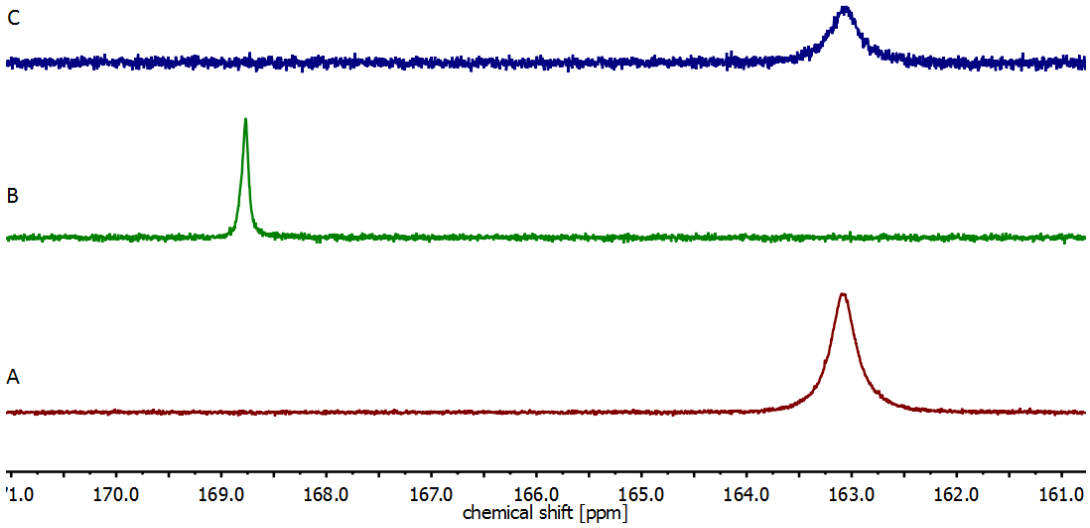

Figure 20: Overview of the $^{31}P\{^{1}H\}$ NMR spectra. Spectrum A is from the free ligand. Five minutes after adding the metal precursor at r.t. spectrum B was obtained. Spectrum C was obtained after 16 h of heating the mixture.

The ratio of the metal precursor is increased and therefore both 3*H*-1,2,3,4-triazaphosphole arms can coordinate to one copper atom (Scheme 23). In Figure 20, only one singlet is observed. To prove coordination, the complex was heated for 16 h at T = 60 °C. The obtained $^{31}P\{^{1}H\}$ NMR spectrum showed only one resonance, assigned to the free ligand. Several unsuccessful crystallization attempts were performed.

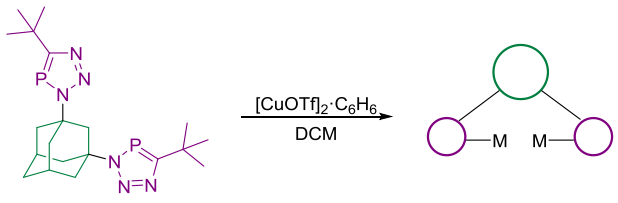

32

Scheme 23: Schematic representation of what kind of complex might be formed.

Triphenylphosphine oxide was again used as internal standard to verify the formation of a complex. The standard was added to ligand **32** and metal precursor in solution. The difference in chemical shift was Δδ = 136.4 ppm. This shift was also not significantly larger than the Δδ = 135.7 ppm difference between the ligand **32** and internal standard.

For both the 2:1 and 1:1 ratio complexation reactions, a downfield shift in $^{31}P\{^{1}H\}$ NMR spectroscopy was obtained. A singlet at δ = 167.5 ppm was observed for the 2:1 ratio ratio, while a signal at δ = 168.8 ppm for the 1:1 ratio.

CuBr·SMe_2 was used as a different Cu(I) source. Different ratios between ligand **32** and the copper precursor were used. Figure 21 showed an overview of the obtained $^{31}P\{^{1}H\}$ NMR spectra. Spectrum A shows the chemical shift of the free ligand and spectrum B is obtained after the addition of the copper precursor (1:1 ratio). Increasing the amount of metal precursor to a 1:2 ratio gave spectrum C. For the 1:1 ratio, two signals appeared upon coordination of one copper atom to the ligand. When the ligand acted in a bidentate fashion, only one signal was obtained by $^{31}P\{^{1}H\}$ NMR spectroscopy. Since the same spectrum was obtained for the 1:2 ratio, presumably no coordination occurred in both cases.

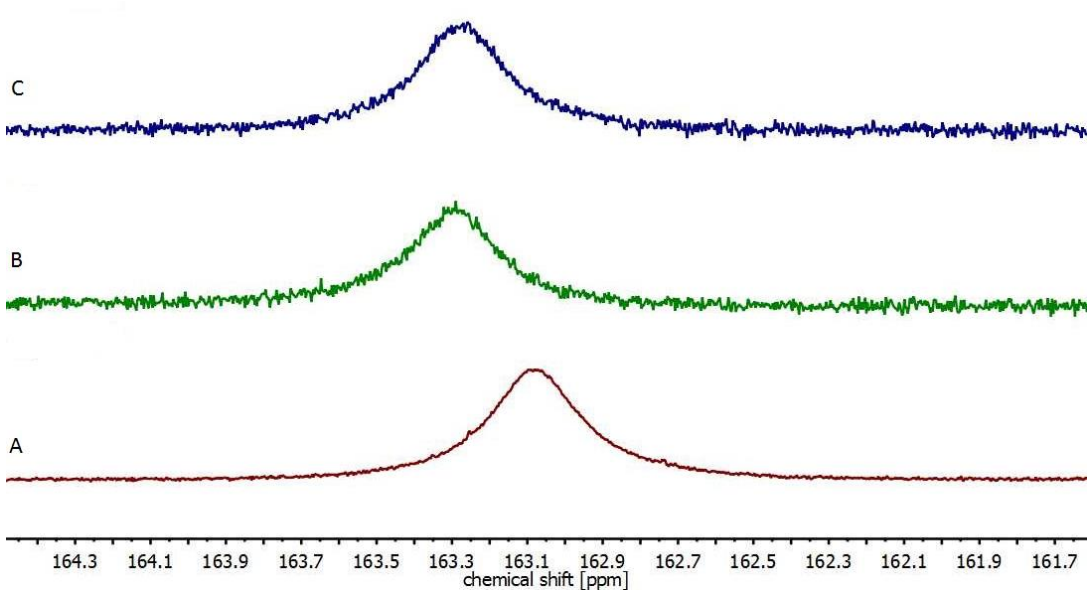

Figure 21: Overview of the $^{31}P\{^{1}H\}$ NMR spectra. Spectrum A is from the free ligand. Adding the metal precursor in a 1:1 ratio gave spectrum B. Spectrum C was obtained when a 1:2 ratio was used. Both reactions were measured by $^{31}P\{^{1}H\}$ NMR spectroscopy after 5 minutes when the metal precursor was added at room temperature.

Attempts in coordination chemistry with Au(I)

Only one gold metal precursor was used: AuCl·SMe_2. Both a 1:1 ration of compound **32**: AuCl·SMe_2 and a 1:2 ratio of compound **32**:AuCl·SMe_2 samples were prepared. They were protected from light, since the gold precursor is light sensitive. Furthermore, they were monitored using $^{31}P\{^{1}H\}$ NMR spectroscopy. First, the 1:1 ratio will be discussed.

Figure 22 showed an overview of the obtained spectra. When the metal precursor was added to the ligand, a small downfield shift in $^{31}P\{^{1}H\}$ NMR spectroscopy was obtained (spectrum B). The metal precursor was poorly soluble in DCM, so the mixture was heated for 16 h (spectrum C). The same chemical shift was obtained as for the free ligand (spectrum A). This might indicate that a complex was formed, but decomposed during heating. When increasing the reaction time for another 2 days the same signal was obtained as for the free ligand (spectrum D).

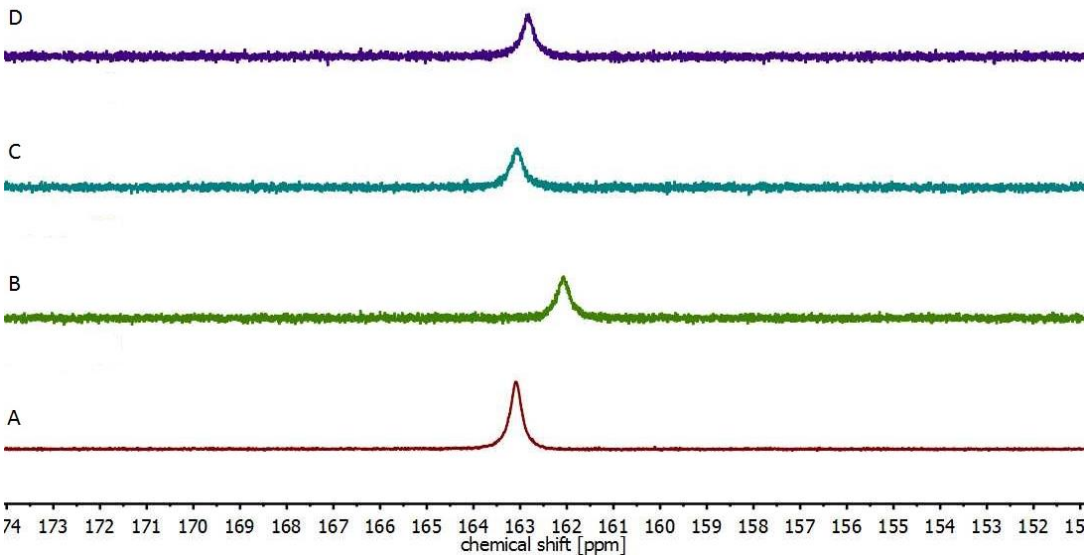

Figure 22: Overview of the obtained $^{31}P\{^{1}H\}$ NMR spectra. Spectrum A belongs to the free ligand. The other three spectra belong to the complexation reaction where a 1:1 ratio of ligand 32:AuCl·SMe_2ratio was used. In spectrum B, the gold precursor was added. Heating the mixture for 16 h gave spectrum C. Increasing the reaction time for 2 days gave D.

According to the HASB concept, gold prefers to coordinate to a phosphorus atom rather than to a nitrogen atom. When coordination occurs, a significant shift in $^{31}P\{^{1}H\}$ NMR spectroscopy would be expected. This does not occur in Figure 22. It is unlikely that a complex was formed.

Figure 23 shows an overview of the obtained $^{31}P\{^{1}H\}$ NMR spectra when a 1:2 ratio of the ligand to metal precursor was used. Spectrum B shows, just as for the 1:1 ratio, a small upfield shift. The solubility was poor and therefore this mixture was also heated for 16 h at T = 60 °C. Here, the signal shifted to the same chemical shift as that of the free ligand. Furthermore, a new singlet at δ = -41.16 ppm occurred (spectrum C), which might indicate that a new species is formed. Increasing the reaction time for another 2 days gave spectrum D. Here, the intensity of the signal at δ = -41.16 ppm did not increase or decrease.

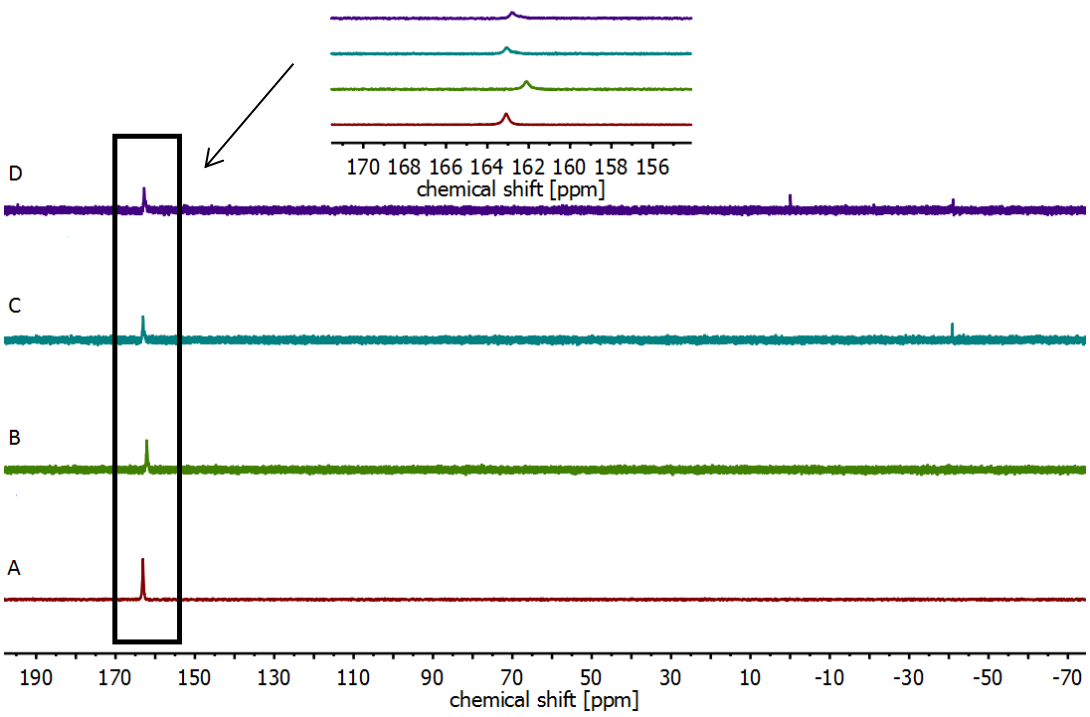

Figure 23: Overview of the obtained $^{31}P\{^{1}H\}$ NMR spectra. Spectrum A belongs to the free ligand. The other three spectra belong to the complexation reaction where a 1:2 ratio of ligand 32:AuCl·SMe_2 was used. In spectrum B, the gold precursor was added. Heating the mixture for 16 h gave spectrum C. Increasing the reaction time for 2 days gave D.

The shifts that occurred around δ = 163 ppm were comparable in Figure 22 and 23. Heating the reaction mixture showed an upfield shift compared with the free ligand. Increasing the reaction time resulted in the same chemical shift as for the free ligand. Increasing the reaction time for another 2 days also showed the same signal. The only difference was that a new singlet occurred at δ = -30 ppm for the 1:2 ratio. Since both reactions showed similar spectra and gold prefers coordination to the phosphorus atom, it is plausible that no complex was formed in either case.

Attempts in coordination chemistry with Rh(I)

From the metal precursors, which were described in the previous sections, it is difficult to estimate whether there is coordination or not. Therefore the strategy was changed for rhodium. Rhodium has the same nuclear spin as phosphorus, which made it easier to determine whether there is coordination or not. The metal precursor $[Rh(CO)_2Cl]_2$ was used. Using this dimer, a complex **A** (Scheme 24) might be formed. To investigate this possibility, several different set-ups were used.

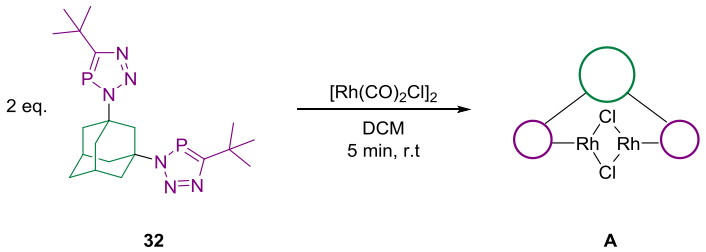

Scheme 24: Schematic representation of the complexation reaction between ligand 32 and the Rh dimer to form complex A.

First, a mixture with a 2:1 ratio of the ligand and Rh-dimer was used. $^{31}P\{^{1}H\}$ NMR spectroscopy revealed a broad singlet at δ = 162.6 ppm and another signal at δ = 175.7 ppm (Figure 24). The broad singlet was upfield shifted compared with the free ligand. The other signal indicates that a complex was formed.

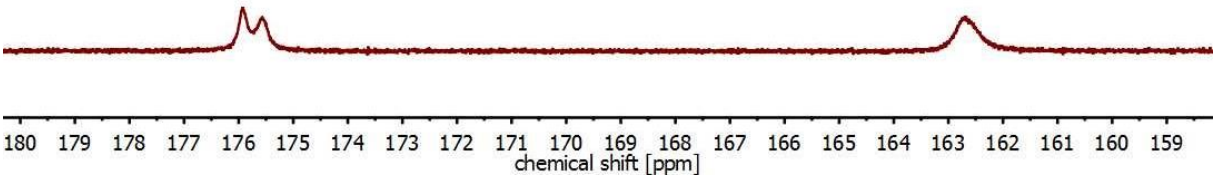

Figure 24: $^{31}P\{^{1}H\}$ NMR spectrum of the complexation reaction between the Rh-dimer and ligand 32 (1:2 ratio).

To obtain more information about the complex, crystallization attempts were performed. Crystals were obtained that were suitable for X-ray analysis. Figure 25 shows the molecular structure of complex **40** in the crystal. The Rh dimer was cleaved and coordinated via the N^1 atom of both 3*H*-1,2,3,4-triazaphosphole arms. Unfortunately, the Rh dimer was not properly stored. Instead of storing it in the freezer, it was stored at room temperature. Therefore, the dimer may already have decomposed before reacting with ligand **32**.

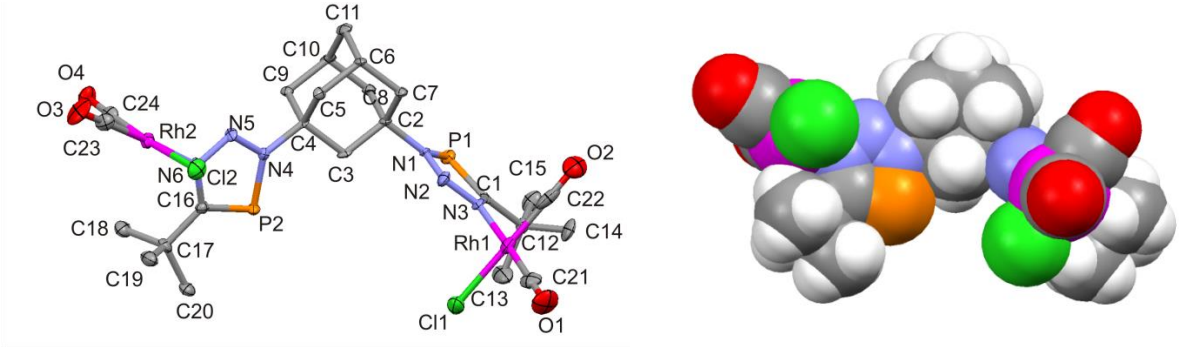

Figure 25: : ORTEP plot of the molecular structure of compound 40 in the crystal. Ellipsoids are shown at the 50 % probability level. Hydrogen atoms are omitted for clarity (left). Space filling of the molecular structure of compound 40 in the crystal (right). Selected bond lengths (Å) and angles (°): Rh(1)-Cl(1) 2.336(6), Rh(1)-N(3) 2.111(2), Rh(1)-C(22) 1.818(1), Rh(1)-C(21) 1.845(2), C(21)-O(1) 1.140(8), C(22)-O(2) 1.170(4), Rh(1)-Cl(1) 2.336(6), Rh(2)-N(6) 2.113(0), Rh(2)-C(24) 1.841(5), Rh(2)-C(23) 1.848(0), Rh(2)-Cl(2) 2.344(6), Rh(2)-N(6) 2.113(0), C(23)-O(3) 1.124(9), C(24)-O(4) 1.145(8), P(2)-C(16) 1.706(1), P(1)-C(1) 1.724(2), C(16)-P(2)-N(4) 87.18, Cl(2)-Rh(2)-N(6) 88.35, C(23)-Rh(2)-N(6) 176.61, N(1)-P(1)-C(1) 86.64, C(21)-Rh(1)-N(3) 176.52

As mentioned before, the Rh dimer dissociates, and each metal atom coordinates via the N^1 of the 3*H*-1,2,3,4-triazaphosphole arms. No carbon monoxide was eliminated during the formation of complex **40**, which gives the metal atom a coordination number of four. The C(23)-Rh(2)-N(6) and C(21)-Rh(1)-N(3) angles are both almost 180°. The Cl(1)-Rh(1)-C(22) and Cl(2)-Rh(2)-C(24) angles are almost 180°. This indicates that the metal atoms are located in a square planar geometry.

Interpretation of the $^{31}P\{^{1}H\}$ NMR spectrum with the obtained molecular structure is still difficult. The signal at δ = 175.7 ppm might be interpreted as two singlets or as a doublet. The 3*H*-1,2,3,4-triazaphosphole arms of complex **40** can rotate, but have a lack of free rotation (Figure 25). Due to

this, the phosphorus atoms have a small difference in chemical environment and therefore two singlets are obtained. The doublet can also be explained by a ^{3}J coupling between the Rh and P atom of 58 Hz, which is not very high. However, Ruiz *et al.* showed the synthesis of rhodium complex, where the rhodium coordinates to a phosphorus atom.[25] Here, a ^{1}J of 128.8 Hz was obtained. The obtained coupling constant might therefore still be high.

In the previous alinea the signal at δ = 175.7 ppm was explained, but not the singlet at δ = 162.6 ppm. This signal is shifted upfield compared to the free ligand. It might be that there is still some free ligand left. Another possibility is that only one metal coordinates to the ligand (Scheme 25). The complex loses the interior mirror image, resulting in the appearance of two signals in $^{31}P\{^{1}H\}$ NMR spectroscopy. One of them is the singlet at δ = 162.6 ppm, which is from the 3*H*-1,2,3,4-triazaphosphole arm without coordinated metal. The other signal could be overlapping with the signal at δ = 175.7 ppm.

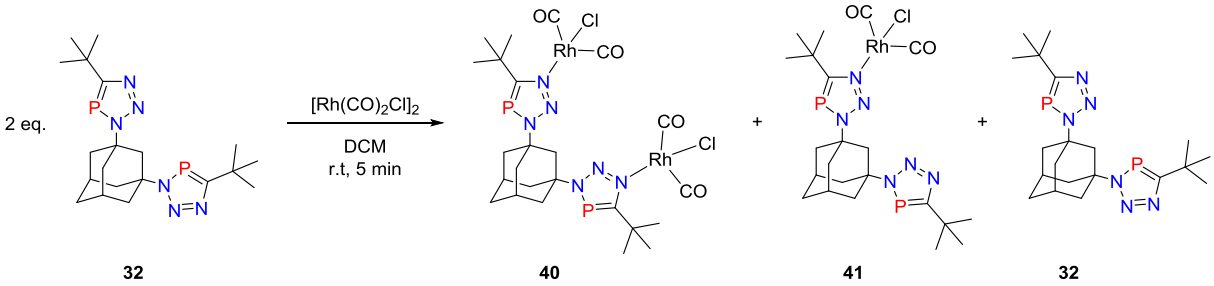

Scheme 25: Overview of the possible compounds obtained during the complexation reaction of ligand 32 and the Rh dimer.

Another complexation reaction was performed with an increased amount of ligand (4:1 ratio of compound **32**:rhodium precursor). The $^{31}P\{^{1}H\}$ NMR spectrum is presented in Figure 26 (spectrum A). The intensity of the singlet at δ = 162.45 ppm increased compared to the signal observed in the spectrum in Figure 24. This indicates that there was still some free ligand left. Furthermore, there could be some coordination of one Rh atom to one of the two 3*H*-1,2,3,4-triazaphosphole arm. The phosphorus atom in the 3*H*-1,2,3,4-triazaphosphole arm without coordinated metal might had peak overlap with the free ligand. The signal at δ = 175.5 ppm was different than in Figure 24. Here, a singlet was obtained, which contained a 'shoulder'. It might be that a different species was formed than for the 2:1 ratio.

The last coordination attempt between the Rh dimer and ligand was performed with a 1:1 ratio. This sample was not concentrated enough, because a high signal-to-noise ratio was obtained (Figure 26 spectrum B). The spectrum consisted, in contrast with the previous experiments, of two singlets. These singlets had roughly the same chemical shift as in the previous experiments. A different complex was likely formed from those seen in the previous complexation reactions.

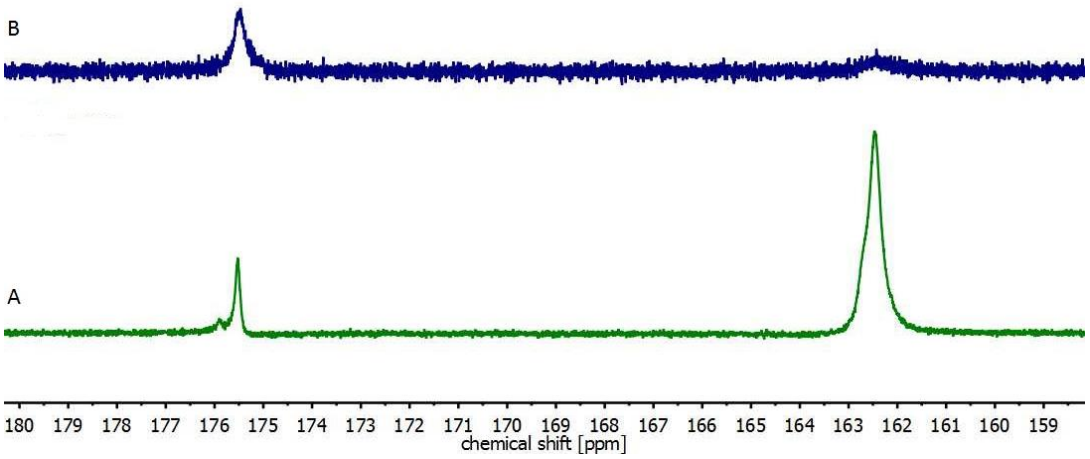

Figure 26: $^{31}P\{^{1}H\}$ NMR spectra of the complexation reaction between the Rh-dimer and ligand 32. Spectrum A shows the 4:1 ratio of compound 32:rhodium precursor. Spectrum B shows the 1:1 ratio between them.

3.4 Coordination chemistry with TMS-TAP 35

Not only the coordination behavior of compound **32** was investigated, but also for compound **35**. Several different metal precursor were used for the complexation reaction with ligand **35**.

Attempts in coordination chemistry with Cu(I)

The coordination chemistry of ligand **35** was also explored. Two different metal precursors were used: $[CuOTf]_2 \cdot C_6H_6$ and $CuBr \cdot SMe_2$. First, the complexation reaction of $[CuOTf]_2 \cdot C_6H_6$ will be discussed. Figure 27 shows an overview of the different complexation reactions that were performed. Spectrum B shows the obtained spectrum of a 2:1 ligand to metal ratio. The signal shifted downfield 4.0 ppm compared to the free ligand (spectrum A). This downfield shift also appeared for the complexation reaction with ligand **32** (Figure 19). Increasing the amount of metal precursor to a 1:1 ratio gave exactly the same chemical shift as in the previous reaction.

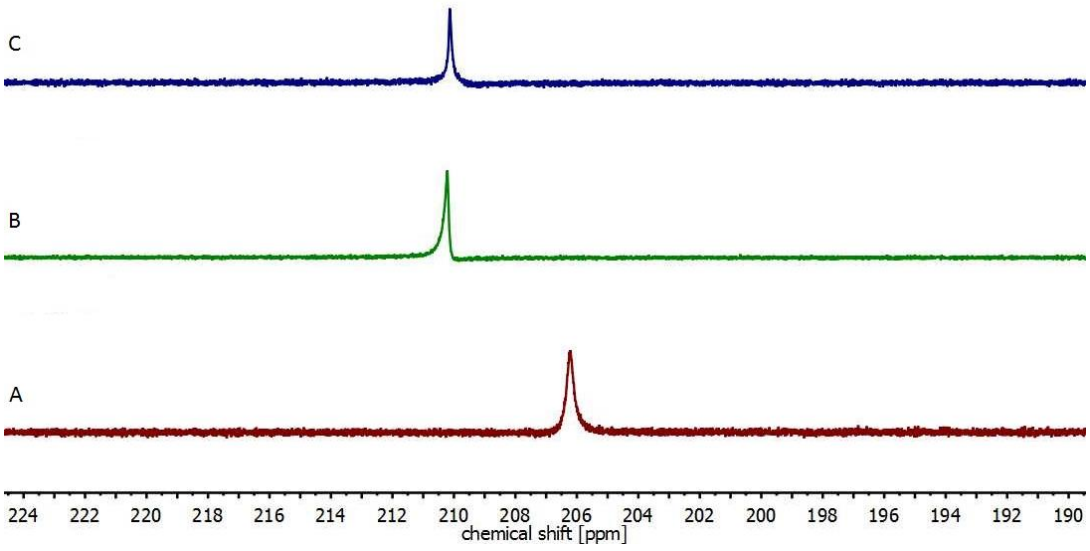

Figure 27: Overview of the obtained $^{31}P\{^{1}H\}$ NMR spectra. Spectrum A belongs to the free ligand. The other two spectra belong to the complexation reaction of ligand 35 and $[CuOTf]_2 \cdot C_6H_6$ as the metal precursor. Spectrum B was measured 5 minutes after adding the copper metal precursor at r.t. in a 2:1 ratio. In spectrum C, the ratio was changed to 1:1.

From these spectra, no estimation can be given on whether coordination occurred. Coordination through only one of the two 3*H*-1,2,3,4-triazaphosphole arms should give two singlets in the $^{31}P\{^{1}H\}$ NMR spectrum. When the ligand acted in a bidentate fashion, only one singlet would be obtained, as in spectrum B. However, when increasing the amount of metal precursor a different complex was expected to be formed. Therefore, no coordination likely occurred in either case. This was verified using an internal standard (triphenylphosphine oxide). The difference in chemical shift between the internal standard and ligand **35** was Δδ = 178.9 ppm. Addition of the metal precursor resulted in a chemical shift difference of Δδ = 178.8 ppm. From these values, it can be concluded that no coordination occurred.

For the 1:2 ratio the same procedure was performed. The standard was added to a mixture of ligand and metal precursor. $^{31}P\{^{1}H\}$ NMR spectroscopy showed a chemical shift difference of Δδ = 178.4 ppm. This value is close to the difference in chemical shift between the ligand and standard. In this experiment, it is difficult to estimate if coordination occurs.

For the $CuBr{\cdot}SMe_2$ precursor, only the 1:1 ratio was investigated. Spectrum A is from the free ligand and spectrum B of the complexation reaction (Figure 28). Here, a small upfield shift of δ = 0.4 ppm was presented. This upfield shift was not obtaining when using ligand **32** (Figure 21 spectrum B).

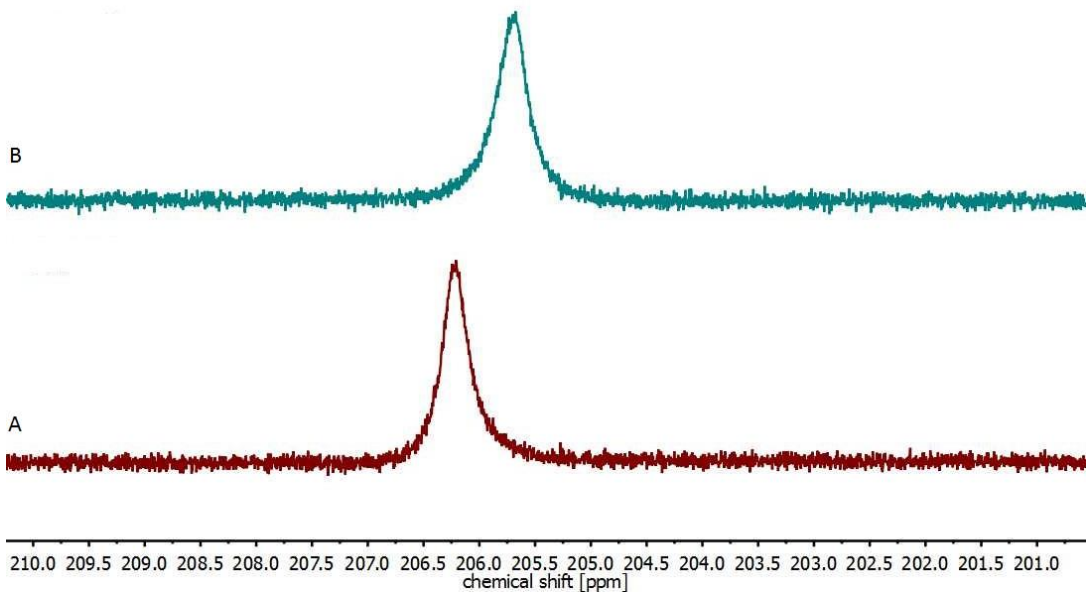

Figure 28: Overview of the obtained $^{31}P\{^{1}H\}$ NMR spectra. Spectrum A is from the free ligand and spectrum B is from the complexation reaction, where a 1:1 ratio was used.

Attempts in coordination chemistry with Rh(I)

Complexation attempts were also performed with the $[Rh(CO)_2Cl]_2$ precursor. Figure 29 showed an overview of the different ratios that were used for complexation. Spectrum B showed the complexation reaction for the 2:1 ligand to metal ratio. Here, a singlet was obtained at δ = 206.0 ppm. This singlet had the same chemical shift as the free ligand (spectrum A). Furthermore, a signal at δ = 215.7 ppm was obtained, which could be better assigned as a doublet rather than two singlets (compared to the obtained spectrum in Figure 24). This resonance can be assigned to the formation

of a metal complex. Although the molecular structure of the crystal could not be obtained, the spectrum shows similar chemical shifts to those for complex **40**. Several crystallisation attempts were performed, but were not successful.

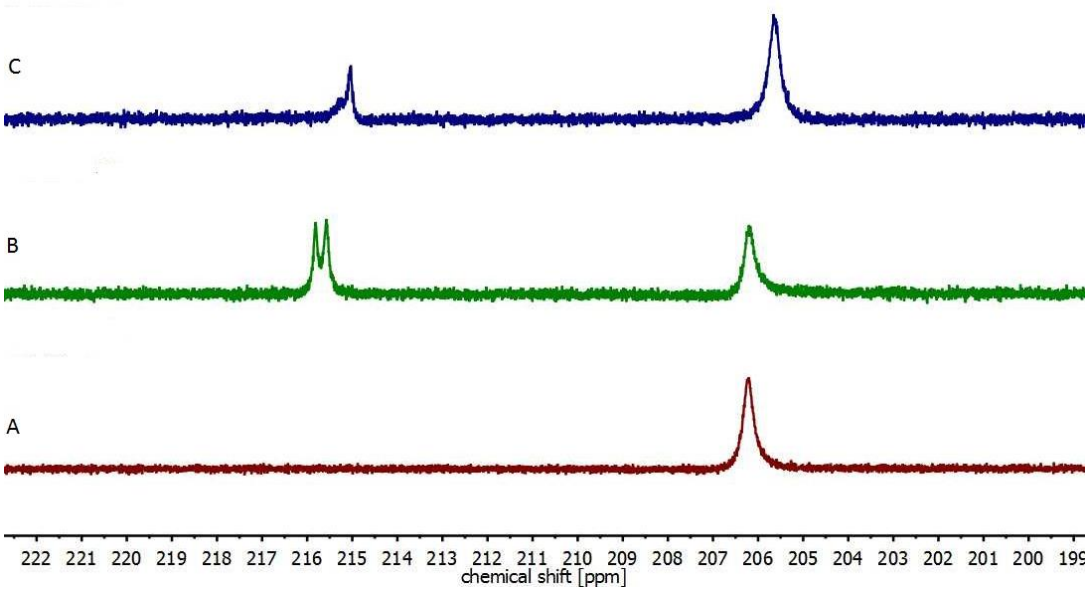

Figure 29: Overview of the obtained $^{31}P\{^{1}H\}$ NMR spectra. Spectrum A belongs to the free ligand. The other two spectra belong to the complexation reaction of ligand 35 and the Rh dimer. In spectrum B, the rhodium precursor was added to a 2:1 = ligand 35:rhodium precursor. In spectrum C the ratio was changed to 1:1.

Scheme 26 shows an overview of the possible complexes. It is plausible that a similar complex is formed compared with complex **40** (Scheme 26 complex **42**). However, since the signal at δ = 215.7 ppm has the shape of a doublet, complex **42** might not be formed. Furthermore, the coupling constants is 38.8 Hz, which is significant lower than the signal obtained in Figure 24. The singlet in spectrum B (Figure 29) is from the 3*H*-1,2,3,4-triazaphosphole arm where no coordination occurs (complex **43**) or from compound **35**, while the doublet is the ^{3}J coupling from the coordinated 3*H*-1,2,3,4-triazaphosphole arm.

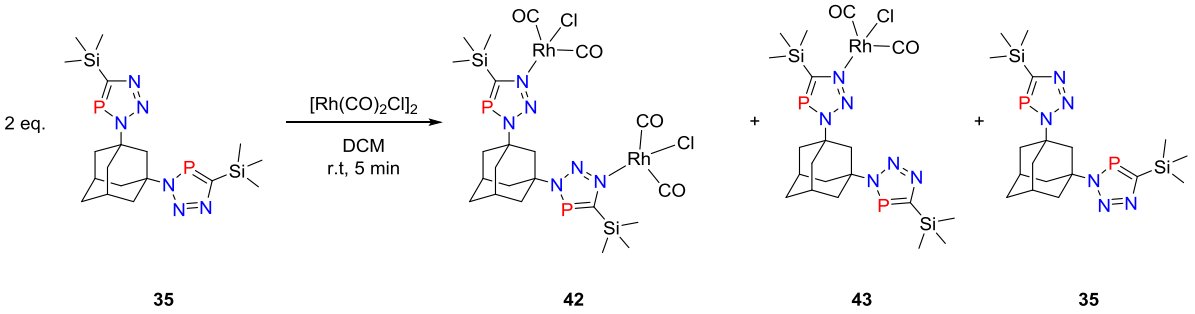

Scheme 26: Overview of the possible obtained compounds during the complexation reaction of ligand 35 and the Rh-dimer.

A 1:1 ratio results in spectrum C. Here, the doublet has vanished and a singlet is obtained with a 'shoulder'. It might be that a different complex was formed in this case than with the 2:1 ratio.

4. Conclusion

In the first part of this project, the desired phosphaalkyne **22** could not be obtained. The reaction pathway to synthesize this compound was not successful, since the procedure was poorly described. The synthesis of phosphaylidene **26** was performed several times with different reaction conditions. Only in one case did this lead to the desired product, but that product could not be purified. The last step in this synthetic pathway was the synthesis of phosphaalkyne **22**. This reaction was also performed by varying several reaction conditions. Monitoring these reactions by means of $^{31}P\{^{1}H\}$ NMR spectroscopy indicated that no product was left at the end of the reaction.

The second part of this project was to synthesize the diazide **23**. Synthesis of the diazide **23** had a high yield of 89 %. Furthermore, it was analyzed by means of IR spectroscopy and ^{1}H NMR spectroscopy. Both confirmed the formation of product. Compound **23** was used for the [3+2] cycloaddition reaction with different phosphaalkynes.

The [3+2] cycloaddition was performed using compound **23** and phosphaalkyne **31**. Compound **32** was obtained in a high yield (>99 %). X-ray diffraction, NMR spectroscopy, IR spectroscopy, and mass spectrometry confirmed the formation of pure product.

Several different metal precursors were used to investigate the coordination chemistry of compound **32**. For the coordination attempts with $[CuOTf]_2 \cdot C_6H_6$ as the metal precursor, not enough information is obtained to prove the formation of a complex. Crystallization attempts were not successful. For the $CuBr \cdot SMe_2$ precursor, no complex is formed; the same spectrum was obtained for a 1:1 ratio of ligand **32**:metal precursor as for the 1:2 ratio.

Similar results were obtained for the $AuCl \cdot SMe_2$ precursor. Performing the reaction in a 1:1 ratio of ligand **32**:metal precursor showed a small shift in the $^{31}P\{^{1}H\}$ NMR spectrum. Heating the reaction at T = 60 °C for several days showed a small shift in the $^{31}P\{^{1}H\}$ NMR spectrum. Increasing the amount of metal precursor to a 1:2 ratio showed the same differences in chemical shift as for the 1:1 ratio, including when the reaction was heated at T = 60 °C for several days. Furthermore, in the case of the 1:2 ratio, a new signal appeared at δ = -41.16 ppm. Increasing the reaction time did not increased the intensity of the signal.

The coordination chemistry was also explored by using $[Rh(CO)_2Cl]_2$ as precursor. Using a ligand to metal ratio of 2:1 showed a small upfield shift compared to free ligand in $^{31}P\{^{1}H\}$ NMR spectroscopy. Furthermore, a new signal at δ = 175.7 ppm was also obtained. Single crystals of the complex were suitable for X-ray diffraction measurements. These measurements show that the Rh dimer dissociates and forms complex **40**. Other ratios for complexation reactions were also performed. The different ratios had different ^{31}P NMR spectra, so different complexes were formed. No crystals of the resulting complexes were obtained for a crystallographic characterization.

Another [3+2] cycloaddition reaction was performed. The reaction between compounds **23** and **34** gave compound **35** in high yield (>99 %). Several analytical techniques confirmed the formation of this product.

Several complexation reactions were performed with compound **35**. The metal precursor $[CuOTf]_2 \cdot C_6H_6$ was used. The 2:1 and 1:1 ratio had the same $^{31}P\{^{1}H\}$ NMR spectrum, which would indicate that no coordination occurred. Furthermore, $CuBr \cdot SMe_2$ was also used. When a 1:1

complexation reaction was performed, an upfield shift was obtained. This was not obtained when the complexation reaction was carried out with compound **32**. Instead, a downfield shift was obtained in $^{31}P\{^{1}H\}$ NMR spectroscopy.

For complexation with rhodium, the Rh dimer $[Rh(CO)_2Cl]_2$ was used. Here, the Rh dimer was not properly stored in the freezer. When a 2:1 ratio was performed a signal at δ = 215.7 ppm and δ = 206 ppm was obtained in the $^{31}P\{^{1}H\}$ NMR spectrum. The signal at δ = 215.7 ppm showed more doublet character compared to when compound **32** was used for complexation (Figure 24 and 29). No crystals were obtained of this complex.

When the amount of metal precursor was increase to a 1:1 ratio, $^{31}P\{^{1}H\}$ NMR spectroscopy was performed. The spectrum was comparable to the complexation with ligand **32**. No crystals were obtained, which were suitable for X-ray diffraction.

The last [3+2] cycloaddition was performed between compound **23** and **36**. Compound **37** was obtained according to $^{31}P\{^{1}H\}$ NMR spectroscopy. Several recrystallization attempts were performed, but were not successful until now. This compound was not used in coordination chemistry.

Compound **32** and **35** were both used as ligands to form new complexes. Different metals and different ratios between the ligand and metal precursor were used. In all cases, these ligands showed no bidentate behavior toward the metal.

5. Outlook

The results obtained in part II are more promising than those of part I. Therefore, it is recommended to continue with part II rather than with part I.

By $^{31}P\{^{1}H\}$ NMR spectroscopy, only a small difference in chemical shift was obtained for the complexation reaction with $CuBr{\cdot}SMe_2$, $AuCl{\cdot}SMe_2$ and $[CuOTf]_2{\cdot}C_6H_6$ compared with the free ligand. This small change in chemical shift is especially true of $[CuOTf]_2{\cdot}C_6H_6$, due to nitrogen coordination. ^{15}N NMR might give more information about whether a new species is formed or not. Furthermore, the analysis techniques mass spectrometry or X-ray diffraction can also be used.

The reactions with the Rh dimer (with ligands **32** and **35**) might be repeated, since the Rh dimer was not stored in the freezer. Further characterization from the reaction using a 2:1 ratio of ligand **32**:rhodium precursor can be performed by IR spectroscopy. Complex **40** should give 2 bands for the CO ligands, due to the internal symmetry of the complex. If complex **41** were obtained, an additional CO band should be observed. Other techniques, like mass spectrometry or X-ray diffraction, can also be used. These recommendations can be used for the other complexation reactions with the rhodium precursor.

Furthermore, the coordination properties could be expanded towards other metal precursors e.g. Ag(I) or Ir(I). These metal precursors can be used for the reaction with ligands **32** and **35**. If all these different metal precursors give no bidentate coordination, then the ligand design should be modified. The two 3*H*-1,2,3,4-triazaphosphole arms might be oriented closer to each other, so that the new ligand might act in a bidentate fashion.

6. Experimental section

All reactions were carried out under an argon atmosphere using standard Schlenk techniques. The chemicals were obtained from commercial sources, unless otherwise is mentioned. Dry solvents were obtained from the solvent purification system SPS-800 from the M. Braun company. The NMR spectra were recorded on a Joel ECX (400 MHz) spectrometer, Joel ECZ (400 MHz) or Bruker AVANCE III (700 MHz). NMR-results are shown in δ (ppm). The ESI-MS spectra were recorded using Agilent 6210 ESI-TOF (4 kV) from the company Agilent Technologies. IR measurements were recorded at a 5 SXC Nicolet FT-IR-Spectrometer with a DTGS detector. Absorption bands are specified in wavenumbers (cm^{-1}).

6.1 Ligand syntheses

Synthesis of compound 27:

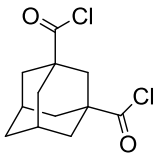

27

A mixture of 1,3-adamantane dicarboxylic acid (1.53 g; 6.81 mmol), $SOCl_2$ (15 mL) and two drops of DMF were refluxed. After 4 h, a clear yellow solution formed, which was cooled to room temperature. Under reduced pressure, the solvent was evaporated. A white solid was obtained. Yield >99 % (quantitative 1.76 g; 6.74 mmol)

The IR values are from compound **27**. ^{1}H NMR was measured of the ethyl ester of compound **27**. Ethanol was added to compound **27**. Removal of the excess of solvent was performed under reduced pressure.

FT-IR: 2936, 2915, 2864, 1787, 1777, 1769 cm^{-1}

^{1}H NMR (400 MHz, $CDCl_3$): 4.11 (q, 4H), 2.15 (m, 2H), 2.02 (s, 2H), 1.85 (m, 8H), 1.68 (m, 2H), 1.24 (t, 6H)

Synthesis of compound 26:

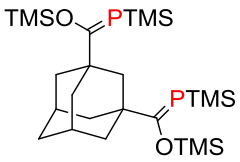

26

Attempt I:

To compound **27** (1.66 g; 6.37 mmol), 29 mL pentane was added, which did not give a clear solution. This mixture was added dropwise to a solution of $P(TMS)_3$ (3.62 g; 14.43 mmol) and pentane (3 mL), which became yellow. The mixture was monitored by $^{31}P\{^{1}H\}$ NMR spectroscopy during 44 h of refluxing. Compound **26** was obtained. Recrystallization by cooling down a hot pentane solution gave no pure product.

Attempt II:

The reaction above was repeated on larger scale. To compound **27** (7.83; 0.03 mol), 20 mL pentane was added, which did not give a clear solution. An ice bath was placed under the Schlenk while adding the $P(TMS)_3$ (16.57 g; 0.07 mol) dropwise. The reaction mixture was monitored by means of $^{31}P\{^{1}H\}$ NMR spectroscopy. Heating the reaction mixture at T = 50 °C for 48 h showed no product in the $^{31}P\{^{1}H\}$ NMR spectrum. DCM (15 mL) was added to the reaction mixture, which was heated again

for 64 h at T = 50 °C, but no product formation could be observed. Increasing the reaction temperature to T = 80 °C for 48 h also showed no product formation.

Attempt III

Compound **27** was not soluble in hexane even upon heating or dilution. Hexane (4 mL) was added to compound **27** (0.54 g; 2.06 mmol). To improve solubility, the mixture was heated to T = 70 °C while adding dropwise a mixture of $P(TMS)_3$ (2.19 g; 8.74 mmol) and hexane (1.4 mL). The mixture was refluxed for 16 h. Analysis by $^{31}P\{^1H\}$ NMR spectroscopy showed only the resonance of the starting material $P(TMS)_3$ and no product formation.

Attempt VI

$Li(TMS)_2 \cdot 2$ THF (1.00 g; 3.06 mmol) (which was not obtained from commercial suppliers) was dissolved in THF (2.5 mL). This solution was added dropwise to a solution of compound **27** (0.36 g; 0.09 mmol) in THF (5.5 mL). The reaction flask was covered with aluminum foil and stirred for 48 h at room temperature. Analysis by $^{31}P\{^1H\}$ NMR spectroscopy showed no product signal.

Attempt V

Dry THF (ca. 15 mL) was added via trap-to-trap distillation to a mixture of compound **27** (0.36 g; 1.39 mmol) and $LiP(TMS)_2 \cdot 2$ THF (1.15 g; 3.06 mmol). The reaction mixture was protected from light and stirred for 16 h at room temperature. The solvent was removed by vacuum distillation. The brown residue and yellow distillate were analyzed by means $^{31}P\{^1H\}$ NMR spectroscopy, showing that no product was formed.

Synthesis of compound 22:

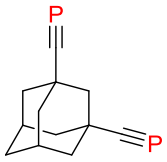

22

Attempt I:

Half of the product mixture obtained from attempt I was dissolved in 3 mL DME with an excess of NaOH and stirred for 16 h at room temperature. The reaction was monitored using $^{31}P\{^1H\}$ NMR spectroscopy. Heating for 2 d at T = 30 °C gave a mixture of product and several byproducts. The reaction was stirred for another 7 days at room temperature. Purification by means of trap-to-trap distillation gave no pure product. Further purification by column chromatography (SiO_2, DCM, air) yielded in decomposition of the product.

Attempt II:

In a second attempt, consuming the other half of the product mixture obtained in attempt I, (1.13 g; 28.3 mmol) NaOH were added. The mixture was heated at T = 125 °C for 2 h in vacuum strip of and volatile products of the reaction mixture. Analysis by means of $^{31}P\{^1H\}$ NMR spectroscopy showed signals of the product, but also resonances of the starting material. The reaction was treated with additional NaOH (1.13 g; 28.3 mmol) and heated to T = 125 °C for 3 h in the trap-to-trap distillation. The $^{31}P\{^1H\}$ NMR spectrum showed that the signal for the product vanished.

Synthesis of compound 23:[21]

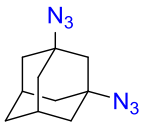

23

A mixture of 1,3-dibromoadamantane (1.13 g; 3.4 mmol), azidotrimethylsilane (3 mL; 22.6 mmol), $SnCl_4$ (0.8 mL; 6.8 mmol) and DCM (13 mL) were degassed for 10 minute and refluxed for 3 d. After the reaction mixture was allowed to cool down to r.t., it was poured into an ice bath and stirred for 30 minutes, followed by an extraction procedure, starting with with Et_2O and H_2O, saturated $NaHCO_3$ and brine. The organic phase was dried over $MgSO_4$ and filtered. The solvent was removed in vacuo and purification of the crude product was performed by plug column chromatography (SiO_2, Et_2O). The solvent was removed under reduced pressure. A white solid was obtained and stored at T = -20°C. Yield 89.0 % (0.74 g; 3.0 mmol)

^{1}H NMR (400 MHz, $CDCl_3$): 2.37 (bs, 2H), 1.84-1.69 (m, 10H), 1.42 (s, 2H)

FT-IR: 2930, 2857, 2084, 1350, 1249 and 1072 cm^{-1}

Synthesis of compound 32:

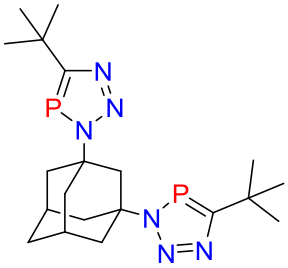

32

To compound **23** (0.50 g; 2.31 mmol) an excess of phosphaalkyne **31** dissolved in THF was transferred by a trap-to-trap distillation. The mixture was allowed to warm up to r.t. and stirred for additional 24 h. Removal of the excess of compound **31** and the solvent was performed by trap-to-trap distillation. A white solid was obtained. Yield >99 %, (quantitative 0.49 g; 2.28 mmol). Single crystals suitable for X-ray diffraction were obtained by recrystallisation from a hot saturated solution in hexane solution.

^{1}H NMR (700 MHz, CD_2Cl_2): 2.90 (s, 2H), 2.63 (s, 2H), 2.50 (d, $J_{H\text{-}H}$=13.4 Hz, 4H), 2.43 (d, $J_{H\text{-}H}$=10.9 Hz, 4H), 1.92 (s, 2H), 1.48 (s, 18H).

^{13}C NMR (700 MHz, CD_2Cl_2): 196.3 (d, $^1J_{C\text{-}P}$= 55.6 Hz), 63.5 (d, $^2J_{C\text{-}P}$=6.2 Hz), 52.7, 44.6 (d, $^3J_{C\text{-}P}$=6.5 Hz), 35.6, 35.3, 31.9, 31.4, 1.4.

^{31}P{^{1}H} NMR (400 MHz, CD_2Cl_2): 163.2 (s).

FT-IR: 2964, 2930, 2854, 1262, 1017 and 803 cm^{-1}.

ESI-TOF (m/z): calculated $[M+H]^+$: 419.2260 found m/z 419.2242, calculated $[M+Na]^+$: 441.2056 found m/z 441.2082, calculated $[M+K]^+$: 457.1795 found m/z 457.1843

Synthesis of compound 34:[26]

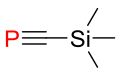

34

Dichloro((trimethylsilyl)methyl)phosphane (which was not obtained from commercial suppliers) (3.43 g; 18.14 mmol), DABCO (4.48 g; 39.90 mmol) and AgOTf (10.30 g; 40.09 mmol) were suspended in 140 mL dry toluene. The mixture was stirred under the exclusion of light for 1 h at r.t. Vacuum distillation was performed, which gave a colorless liquid. The product was obtained in a toluene solution.

^{31}P{^{1}H} NMR (400 MHz, no solvent): 98.8 (s).

Synthesis of compound 35:

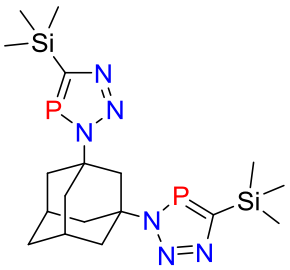

35

Compound **34** dissolved in toluene was added by trap-to-trap distillation to 0.55 g (2.51 mmol) of compound **23**. The mixture was stirred for 24 h at T = -20 °C. Removal of the solution was performed by trap-to-trap distillation. A white solid was obtained, which was recrystallized by cooling down a hot saturated solution in pentane. Yield >99% (quantitative 1.12 g; 2.48 mmol)

^{1}H NMR (700 MHz, CD_2Cl_2): 2.92 (s, 2H), 2.61 (s, 2H), 2.49 (d, $J_{H\text{-}H}$=13.4 Hz, 4H), 2.43 (d, $J_{H\text{-}H}$=11.9 Hz, 4H), 1.90 (s, 2H), 0.38 (s, 18H)

^{13}C NMR (700 MHz, CD_2Cl_2): 182.3 (d, $^{1}J_{C\text{-}P}$=74.0 Hz), 63.2 (d, $^{2}J_{C\text{-}P}$=5.6 Hz), 52.8, 44.6 (d, $^{3}J_{C\text{-}P}$= 5.6 Hz), 34.9, 31.2, 22.4, 14.1, 1.0

^{31}P{^{1}H} NMR (400 MHz, CD_2Cl_2): 206.6 (s)

FT-IR: 2955, 2930, 1934, 1252, 950, 840 cm^{-1}

ESI-TOF-(*m/z*): calculated $[M+H]^+$: 451.1780 found m/z 451.1801.

Synthesis of compound 37:

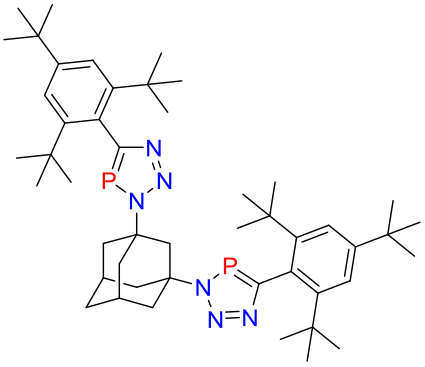

37

Compound **36** (which was not obtained from commercial sources) (0.0980 g; 0.34 mmol), compound **23** (0.068 g; 0.23 mmol) were dissolved in 5 mL dry DCM. The mixture was stirred for 16 h at r.t. and monitored by means of ^{31}P{^{1}H} NMR spectroscopy. Since only starting material was observed, the reaction mixture was heated to T = 40 °C for 16 h. After the solvent was removed, recrystallisation attempts were performed. Recrystallisation from a hot saturated solution in hexane or pentane gave no pure compound.

6.2 Complexation reaction

Complexation reactions are prepared in the glovebox and performed in a J.R. Young NMR tube. Gold metal precursors were protected from light. Table 1 shows an overview of the complexation reactions between ligand **32** and the different metal precursors. Table 2 summarizes the results of the coordination attempts with ligand **35**.

Table 1: Coordination attempts of compound **32**.

Reaction	Metal precursor	Ligand **32** (g)	Metal precursor (g)	Ratio Metal:Ligand (mol:mol)	Solvent	$^{31}P\{^{1}H\}$ NMR (in ppm) (r.t, 5 min)
1	$[CuOTf]_2 \cdot C_6H_6$	0.010	0.007	1:2	CD_2Cl_2	167.52 (s)
2	$[CuOTf]_2 \cdot C_6H_6$	0.010	0.014	1:1	CD_2Cl_2	168.77 (s)
3	$CuBr \cdot SMe_2$	0.010	0.005	1:1	CD_2Cl_2	163.29 (s)
4	$CuBr \cdot SMe_2$	0.010	0.010	2:1	CD_2Cl_2	163.30 (s)
5	$AuCl \cdot SMe_2$	0.010	0.007	1:1	CH_2Cl_2	162.09 (s)
6	$AuCl \cdot SMe_2$	0.010	0.014	2:1	CH_2Cl_2	162.09 (s)
7*	$[Rh(CO)_2Cl]_2$	0.040	0.019	1:2	CH_2Cl_2	See Figure 24
8	$[Rh(CO)_2Cl]_2$	0.010	0.010	1:1	CH_2Cl_2	See Figure 26 B
9	$[Rh(CO)_2Cl]_2$	0.080	0.019	1:4	CH_2Cl_2	See Figure 26 A

*Crystals were obtained from THF with pentane as the counter solvent.

Table 2: Coordination attempts of compound **35**.

Reaction	Metal precursor	Ligand **35** (g)	Metal precursor (g)	Ratio Metal:Ligand (mol:mol)	Solvent	$^{31}P\{^{1}H\}$ NMR (in ppm) (r.t, 5 min)
10	$[CuOTf]_2 \cdot C_6H_6$	0.040	0.022	2:1	DCM	210.13 (s)
11	$[CuOTf]_2 \cdot C_6H_6$	0.040	0.045	1:1	DCM	210.15 (s)
12	$[Rh(CO)_2Cl]_2$	0.020	0.009	2:1	DCM	See Figure 29 B
13	$[Rh(CO)_2Cl]_2$	0.020	0.004	1:1	DCM	See Figure 29 C
14	$CuBr \cdot SMe_2$	0.020	0.009	1:1	DCM	205.70 (s)

7. Acknowledgment

First of all, I would like to thank Prof. Dr. Christian Müller for giving me the opportunity to do my internship in his group. I learned a lot during these months in Berlin, working in a different group, university and field in which I had never worked before. Second, I would like to thank Prof. Dr. Bert Klein Gebbink and Dr. Marc-Etienne Moret for being my supervisors from the Utrecht University.

I would also like to thank the whole AK Müller group for their help and support in the lab. In particular, I would like to thank in particular my labmate Julian for his help in the lab and of course for measuring my crystals. I would also like to thank Martin for the compounds I 'borrowed' from him. Last but not least, I would like to thank Antonia for her help with the NMR.

References

(1) Corbridge, D. E. C. *Phosphorus: Chemistry, Biochemistry and Technology*; 2013.

(2) Crabtree, R. . *The Organometallic Chemistry of the Transition Metals*; 2009.

(3) Le Floch, P. *Coord. Chem. Rev.* **2006**, *250*, 627–681.

(4) Sklorz, J. A. W.; Müller, C. *Eur. J. Inorg. Chem.* **2016**, 595–606.

(5) Waluk, J; Klein, H.-P; Ashe III, A. J; Michl, J. *Organometallics* **1989**, *8*, 2804-2808.

(6) Huisgen, R. *Proc. Chem. Soc.* **1961**, 357–369.

(7) Rostovtsev, V. V.; Green, L. G.; Fokin, V. V.; Sharpless, K. B. *Angew. Chem. Int. Ed.* **2002**, *41*, 2596–2599.

(8) Boren, B.C.; Narayan, S.; Rasmussen, L.K.; Zhang, L.; Zhao, H.; Lin, Z.; Jia, G.; Fokin, V. V. *J. Am. Chem. Soc.* **2008**, *130*, 8923–8930.

(9) Himo, F.; Lovell, T.; Hilgraf, R.; Rostovtsev, V. V.; Noodleman, L.; Sharpless, K. B.; Fokin, V. V. *J. Am. Chem. Soc.* **2005**, *127*, 210–216.

(10) Mézailles, N.; Mathey, F.; Le Floch, P. *Prog. Inorg. Chem.* **2001**, 455.

(11) Nyulászi, L.; Veszprémi, T.; Réffy, J.; Burkhardt, B.; Regitz, M. *J. Am. Chem. Soc.* **1992**, *114*, 9080–9084.

(12) Sklorz, J. A. W.; Hoof, S.; Sommer, M. G.; Weißer, F.; Weber, M.; Wiecko, J.; Sarkar, B.; Müller, C. *Organometallics* **2014**, *33*, 511–516.

(13) Sklorz, J. A. W.; Hoof, S.; Rades, N.; Rycke De, N.; Könczöl, L.; Szieberth, D.; Weber, M.; Wiecko, J.; Nyulászi, L.; Hissler, M.; Müller, C. *Chem. Eur. J.* **2015**, *21*, 11096–11109.

(14) Choong, S. L.; Nafady, A.; Stasch, A.; Bond, A. M.; Jones, C. *Dalt. Trans.* **2013**, *42*, 7775–7780.

(15) Choong, S. L.; Jones, C.; Stasch, A. *Dalt. Trans.* **2010**, *39*, 5774–5776.

(16) Müller, C. *unplublished results*.

(17) Veeck, W.-G. 1,2,4-Diazaphosphole mit Phosphanyl-und Arsanylsubstituenten, Universität Kaiserslautern, 1997.

(18) Allspach, T.; Regitz, M. *Synthesis.* **1986**, 31.

(19) Klaić, L.; Alešković, M.; Veljković, J.; Mlinarić-Majerski, K. *J. Phys. Org. Chem.* **2008**, *21*, 299–305.

(20) Märkl, G.; Sejpka, H. *Tetrahedron Lett.* **1986**, *27* (2), 171–174.

(21) Davis, M. C.; Nissan, D. A. *Synth. Commun.* **2006**, *36*, 2113–2119.

(22) Dillon, K.B.; Mathey, F.; Nixon, J. F. *Phosphorus: The carbon Copy*; 1998.

(23) Müller, C. *unplublished results*.

(24) Roesch, P.; Nitsch, J.; Lutz, M.; Wiecko, J.; Steffen, A.; Müller, C. *Inorg. Chem.* **2014**, *53*, 9855–9859.

(25) Ruiz, J.; Mesa, A. F.; Sol, D. *Organometallics* **2015**, *34*, 5129–5135.

(26) Mansell, S. M.; Green, M.; Kilby, R. J.; Murray, M.; Russell, C. A. *C. R. Chimie* **2010**, *13*, 1073–1081.

Appendix

Full ^{31}P NMR spectra of Figure 11

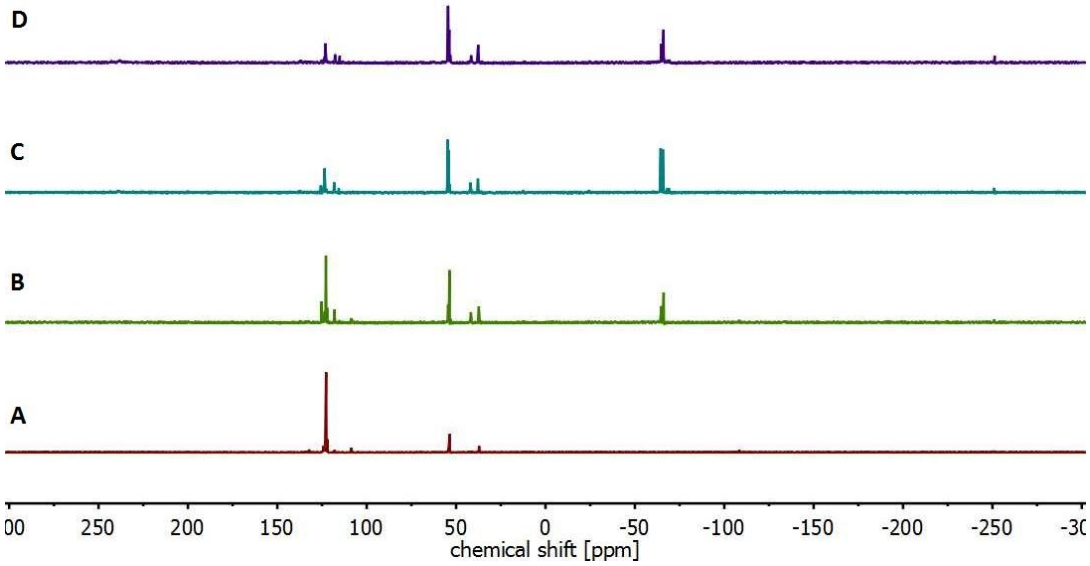

^{1}H NMR of compound 32 measured in CD_2Cl_2

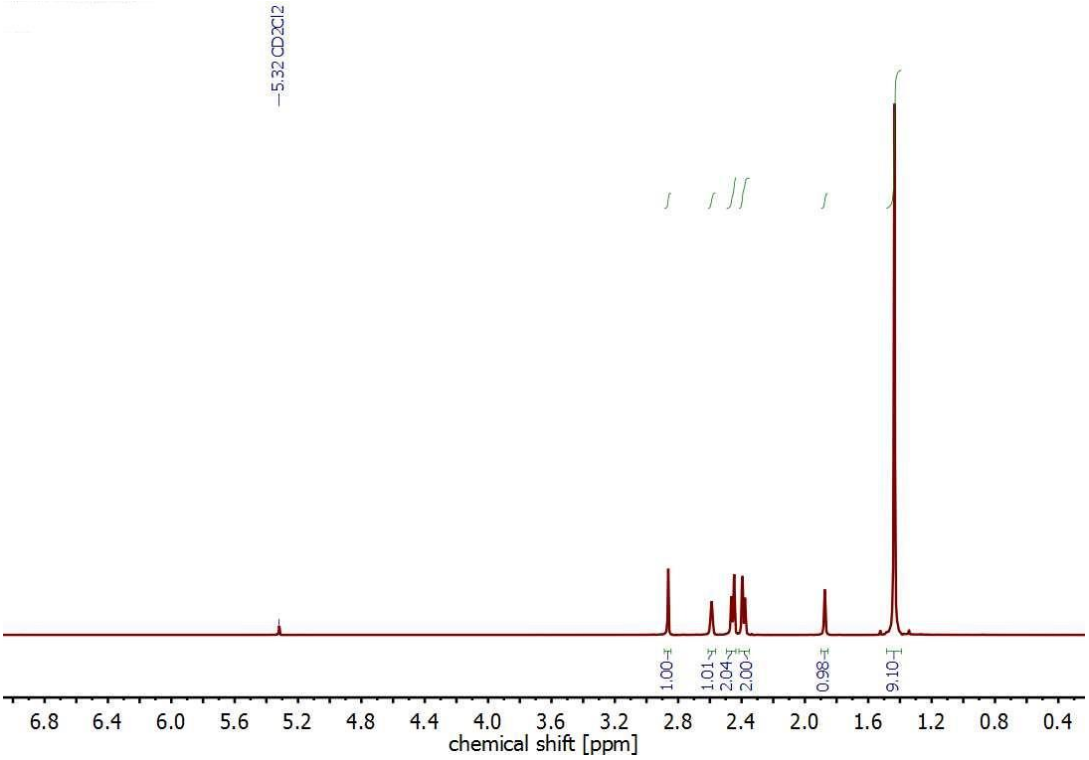

^{13}C NMR of compound 32 measured in CD_2Cl_2

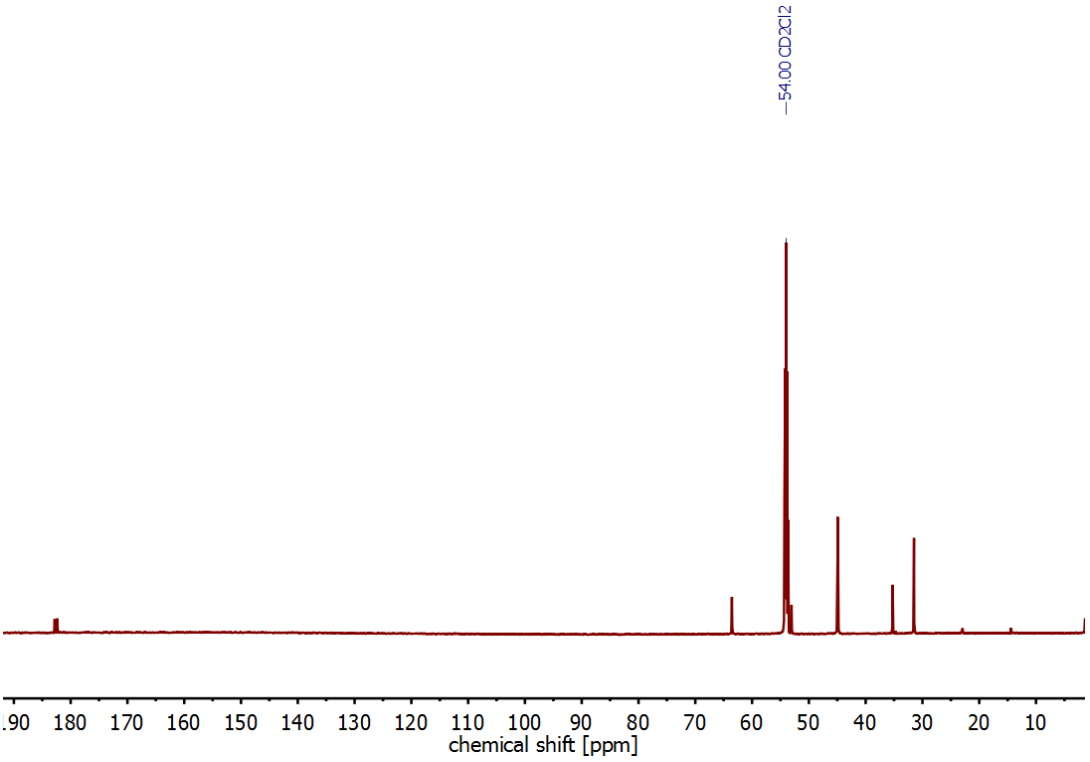

^{31}P NMR of compound 32 measured in CD_2Cl_2

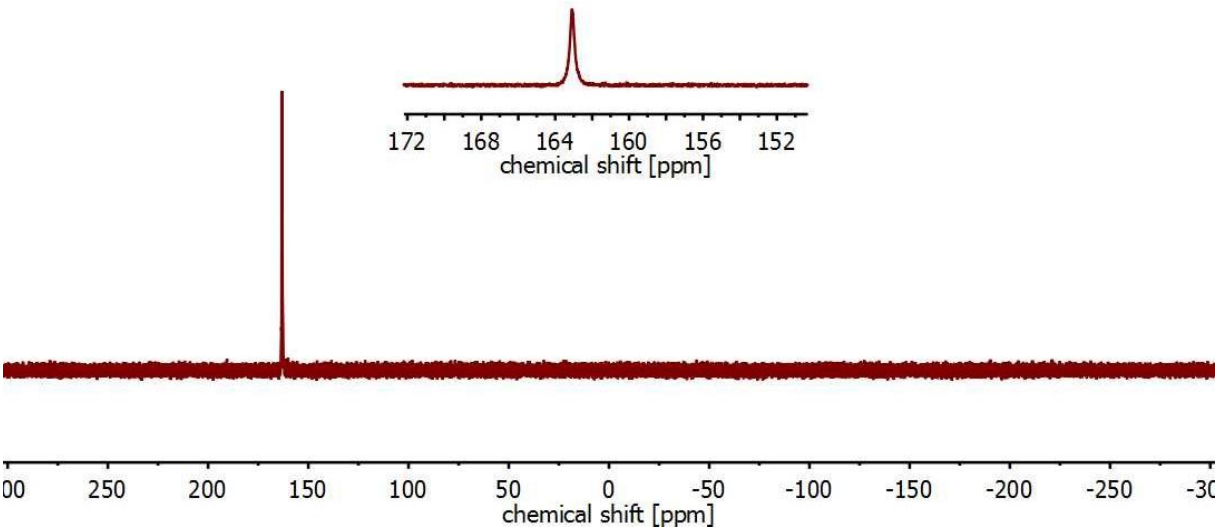

^{1}H NMR of compound 35 measured in CD_2Cl_2

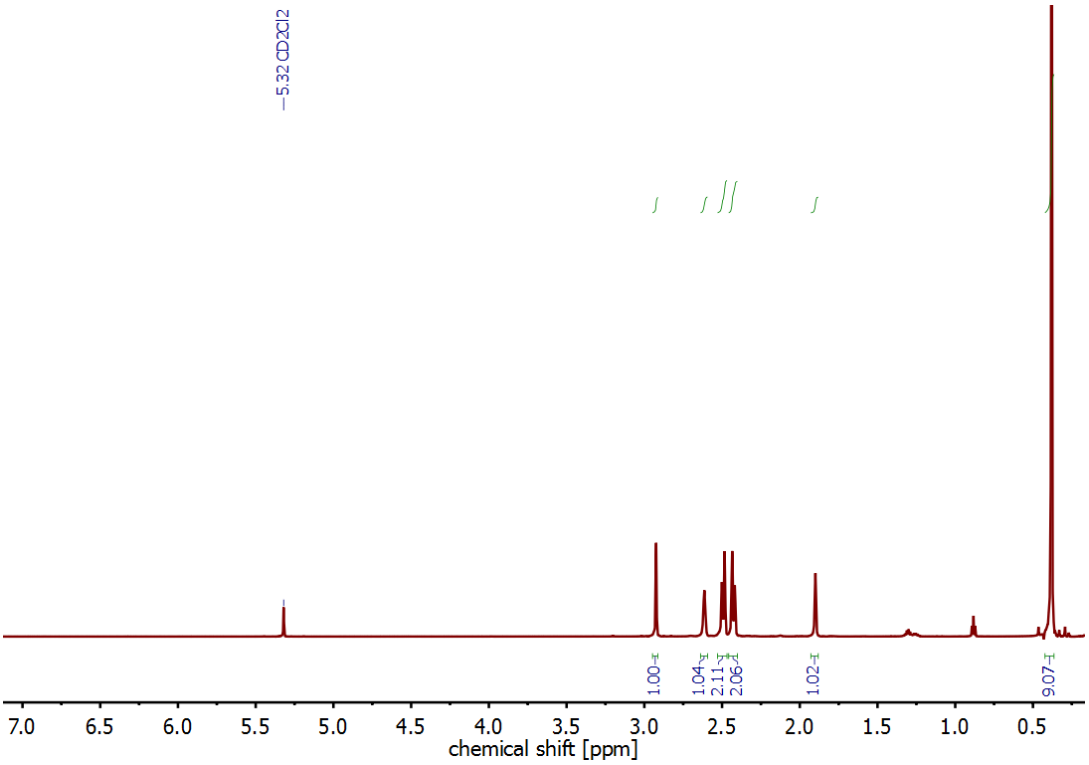

^{13}C NMR of compound 35 measured in CD_2Cl_2

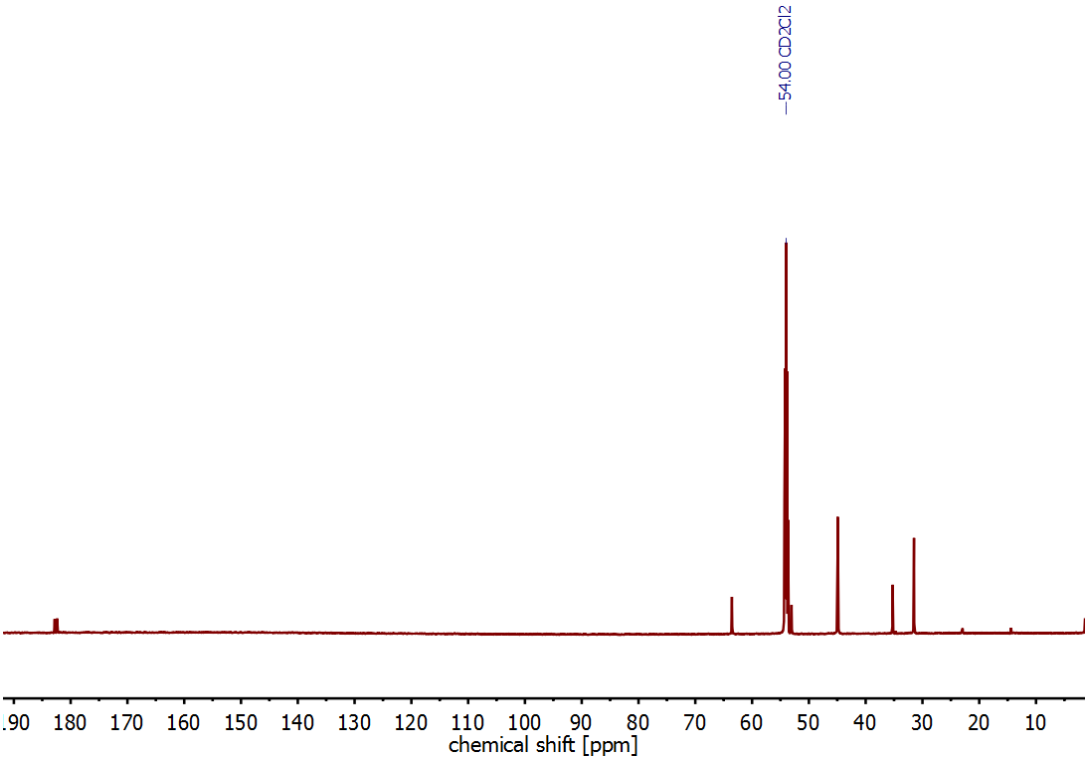

^{31}P NMR of compound 35 measured in CD_2Cl_2

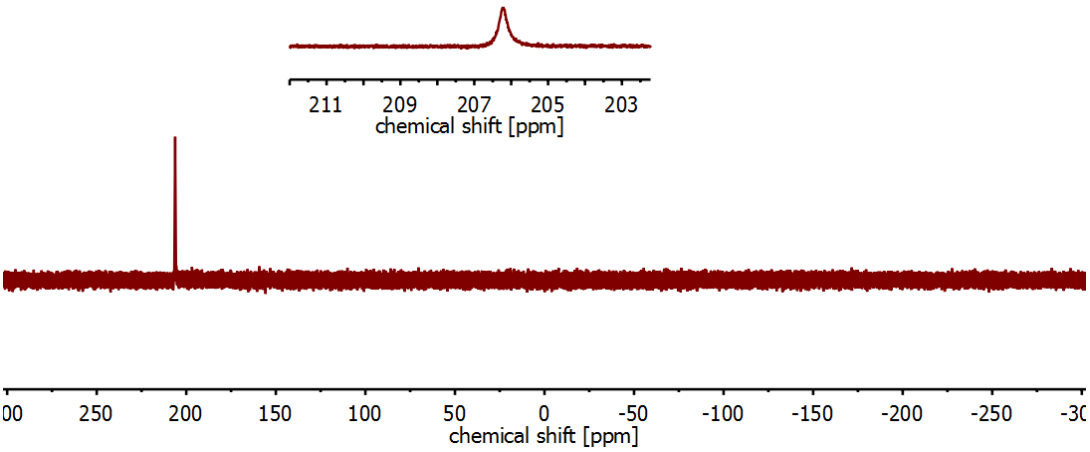

Crystallographic data of compound 32 and 40

	Compound **32**	Complex **40**
Chemical formula	$C_{20}H_{32}N_6P_2$	$C_{24}H_{32}Cl_2N_6O_4P_2Rh_2$
M_z	418.45 g mol^{-1}	807.21 g mol^{-1}
Crystal system	orthorhombic	monoclinic
a (Å)	32.039(7)	16.215(3)
b (Å)	6.5183(14)	16.341(4)
c (Å)	10.492(2)	12.613(2)
β (°)	90	105.276(9)
V (Å)	2191.2(8)	3224.0(12)
Z	4	4
Measured temperature (K)	100(2)	100.0
Absorption correction	multi-scan	multi-scan
Absorption coefficient (mm^{-1})	0.217	1.327
Measured reflections	4234	6646
Independent reflexions	3185	4014
R_1	0.0790(3185)	0.0608(4014)
wR_2	0.1512(4234)	0.1132(6646)
GooF	1.140	1.009